IDEAL TRIANGULATIONS OF 3-MANIFOLDS UP TO DECORATED TRANSIT EQUIVALENCES

RICCARDO BENEDETTI

ABSTRACT. We consider 3-dimensional pseudo-manifolds $\hat{M}$ with a given set of marked point V such that $\hat{M} \setminus V$ is the interior of a compact 3-manifold with boundary. An ideal triangulation T of $(\hat{M}, V)$ has V as set of vertices. A branching (T, b) enhances T to a Δ-complex. Branched triangulations of $(\hat{M}, V)$ are considered up to the b-transit equivalence generated by isotopy and ideal branched moves which keep V pointwise fixed. We extend a well known connectivity result for 'naked' ideal triangulations by showing that branched ideal triangulations of $(\hat{M}, V)$ are equivalent to each other. A pre-branching (T, ω) is a system of transverse orientations at the 2-facets of T verifying a certain global constraint; pre-branchings are considered up to a natural pb-transit equivalence. If M is oriented, every branching (T, b) induces a pre-branching (T, ω_b) and every b-transit induces a pb-transit. The quotient set of pre-branchings up to transit equivalence is far to be trivial; we get some information about it and we characterize the pre-branchings of the type ω_b. Pre-branched and branched moves are naturally organized in subfamilies which give rise to restricted transit equivalences. In the branching setting we revisit, with some complement, early results about the *sliding* transit equivalence and outline a (partially conjectural) conceptually different approach to the branched ideal connectivity and eventually also to the naked one. The basic idea is to point out some structures of differential topological nature on M which are carried by every branched ideal triangulation (T, b) of $\hat{M}$, are preserved by the sliding transits and can be modified by the full branched transits. The *non ambiguos* transit equivalence already widely studied on pre-branchings lifts to a specialization of the sliding equivalence on branched triangulations; we point out a few specific insights, again in terms of carried structures preserved by the non ambiguous and which can be modified by the whole sliding transits.

1. INTRODUCTION

This paper concerns 3-manifold triangulations. The recent article [24] is a fresh and valuable reference for many results about "naked" triangulations (with a lot of expressive pictures). We widely refer to its body and bibliography. We work on a given compact connected smooth 3-manifold M with *non empty* boundary ∂M. We denote by $\hat{M}$ the space obtained by collapsing to one point v each boundary component, we denote V the set of these points. Sometimes $\hat{M}$ is said a *pseudomanifold*. Then the interior $\text{Int}(M)$ is embedded in $\hat{M}$, onto $\hat{M} \setminus V$. The non manifold points of $\hat{M}$ are the points of V associated to non spherical components of ∂M. We consider possibly loose triangulations of $\hat{M}$ such that the set of vertices coincides with V. Sometimes a vertex which is a manifold point is called a *material vertex*. "Loose" means that self and multiple face adjacency are allowed. Such a triangulation is usually called an *ideal triangulation* of $\text{Int}(M)$, understanding that the vertices are "at infinity". This terminology alludes to the triangulations by ideal tetrahedra of a hyperbolic 3-manifold with cusps. However we simply call them ideal triangulations of $\hat{M}$. It is sometimes useful to consider an ideal triangulation as a way to realize $\hat{M}$ by assembling "abstract" tetrahedra by gluing their abstract 2-faces in pairs in such a way that no face remains unglued. Every $\hat{M}$ admits ideal triangulations. The ideal triangulations of $\hat{M}$ are considered up to the *ideal transit equivalence* which is generated by two basic local moves (Section 2) and isotopy which keep V pointwise fixed. These basic *ideal moves* are the $2 \leftrightarrow 3$ and the *quadrilateral* $0 \leftrightarrow 2$ *move*. The numbers in the name refers to the variation of the number of tetrahedra when the move is performed; the move is *positive* if this number increases. Denote by $\mathcal{T}^{id}(M)$ the corresponding quotient set.

The *completed transit equivalence* is obtained by adding one further move called *triangular* $0 \leftrightarrow 2$ *move*. Equivalently we can add instead the *stellar* $1 \leftrightarrow 4$ *move*. In fact we will use freely both moves. After a positive such a move we no longer have an ideal triangulation of $\hat{M}$. Instead we have an ideal triangulation of $\hat{M}'$, where M' is obtained from M by removing the interior of a three ball embedded into $\text{Int}(M)$. So there is a new material vertex in $\hat{M}'$. If such a positive move occurs in a composite transit $T_1 \Rightarrow T_2$ (relative isotopy will be always understood) connecting two ideal triangulations of $\hat{M}$, then it must be compensated later by a negative inverse move. We denote by $\mathcal{T}(M)$ the quotient set under the completed equivalence.

The dual viewpoint. For every ideal triangulation T of $\hat{M}$, the 2-skeleton $\Sigma = \Sigma_T$ of the dual cell decomposition is a *standard* (internal) spine of M. Here "standard" means that the spine has generic singularities and every stratum of its natural stratification is an open cell of the appropriate dimension. Sometimes one says "special" instead of "standard". If we drop out the cellularity condidion, then we have the notion of "simple" spine. A local portion of Σ corresponding to a tetrahedron is called a *butterfly*; the fully symmetric picture of it is the cone based on the 1-skeleton of a tetrahedron with centre at an interior point - one sees it on the left side of Figure 5. The 1-skeleton of Σ is its singular set $\text{Sing}(\Sigma)$. Every 0-cell of $\text{Sing}(\Sigma)$ (also called a vertex) is quadrivalent. The above moves on ideal triangulations can be fully rephrased in terms of standard spines. The spine version of the quadrilateral $0 \leftrightarrow 2$ move is called *lune* move. The spine version of the triangular $0 \leftrightarrow 2$ move is called *bubble* move. We will freely adopt both equivalent dual viewpoints.

Remark 1.1. Although they are equivalent, there is some qualitative difference beetween standard spines and ideal triangulations. For example a triangulation $2 \to 3$ move basically is a *discrete* transition with a cell decomposition as intermediate "state" which is no longer a triangulation. The corresponding spine transition can be realized by a *continuous* deformation passing through a non generic spine. By this difference, sometimes manipulation of spines is easier as more visual.

The naked connectivity results. The following are fundamental well known connectivity results for "naked" triangulations.

Theorem 1.2. *The set $\mathcal{T}(M)$ consists of one point.*

Theorem 1.3. *The set $\mathcal{T}^{id}(M)$ consists of one point.*

A few comments are in order:

(1) These theorems are definitely *weaker* versions of the connectivity results discussed in [24] (Theorem 1.2 and Theorem 1.4 therein respectively). The *strong* versions are obtained by discarding the quadrilateral $0 \leftrightarrow 2$ move from the generators of the completed relation, and also from the ideal relation, provided that one deals with triangulations with at least two tetrahedra.

(2) In both weak and strong versions, Theorem 1.2 obviously is an easy consequence of Theorem 1.3. However, the current proof discussed in [24] of the strong version of the second is based on the validity of the strong version of the first.

(3) In [24] one can find an accurate discussion about the contributions of several authors to the proof of the strong versions of the theorems. The essential ideas to derive the second from the first are due to Matveev [22] and Piergallini [23]; a detailed implementation as a particular case of a more general result is in [3].

(4) The present weak version of the theorems is adequate to our aims for several reasons:

  (a) Since our early motivations by dealing with the quantum hyperbolic invariants, in the decorated setting we are mainly concerned with the opposition *ideal vs completed* transit equivalence, not with the search of a minimal set of generating moves; for example the quadrilateral $0 \leftrightarrow 2$ move occurs very naturally in the treatment of non ambiguous structures carried by layered triangulations of 3-manifolds fibred on S^1 with punctured fibre and their reduced QHI, see [5], [4], [1].

  (b) More substantially, we assume a refinement of Theorem 1.3 (hence of 1.2) in our weak version, due to [20]; for every ideal triangulations T_1 and T_2 of $\hat{M}$, this provides the existence

of composite ideal transits towards a *same* triangulation T, $T_1 \Rightarrow T$, $T_2 \Rightarrow T$, both enterely composed by *positive* ideal moves ($2 \to 3$ *and* $0 \to 2$). Positive moves behave well with respect to their decorated enhancements; see in particular Lemma 2.1 which is our starting point to treat decorated transit equivalences.

Decorated triangulations and their transit equivalences. Different notions of decorated ideal triangulations of 3-manifolds considered up to suitable transit equivalences naturally arise for example in the developments of *quantum hyperbolic geometry*, see in particular [6], [5], [4], and in several other instances of quantum invariants based on some "$6j$ symbols" theory (see [5]); on the other hand, the theme of the combinatorial realization of different kind of structures on M of differential topological nature in terms of suitably decorated triangulations up to transit has been faced since [12] to [8], see also [2], [14], [21]. Here we consider two basic kinds of decoration. Let T be an ideal triangulation of $\hat{M}$ and Σ be the dual spine of M.

- **Branching:** A branching b on T is a system of orientations of the edges of T which lifted to every abstract tetrahedron (Δ, b) of T is induced by a (local) ordering of the vertices, so that every edge goes towards the bigest endpoint. Equivalently b enhances T to be a Δ-*complex* accordingly with [17], Chapter 2. Usually an order of the verices of Δ will be specified by a labelling by $0, 1, 2, 3$. Dually (T, b) becomes (Σ, b) (we keep the notation b) that is a system of transverse orientations of the open 2-cells of Σ (also called regions).

  M oriented: In this case (Σ, b) is equivalent to a system of orientations of the regions, by stripulating that every b-oriented edge of (T, b) intersects its dual oriented region with intersection number equal to 1. Then the branching condition translates in the property that at every open 1-cell e in $\mathrm{Sing}(\Sigma)$ (also called an edge) the three incident local branches of oriented regions of (Σ, b) do not induce the same orientation on e; hence there is a *prevailing orientation* induced by two of them. If M is oriented, to every branched ideal triangulation (T, b) is associated a simplicial fundamental 3-cycle

$$Z(T, b) := \sum_{\Delta \subset T} *_{(\Delta, b)} (\Delta, b)$$

where (Δ, b) varies among the 3-simplexes of the Δ-complex (T, b), the sign $*_{(\Delta, b)} = \pm 1 \in \mathbb{Z}$ and equals 1 if and only if the b-orientation of Δ agrees with the ambient orientation of M.
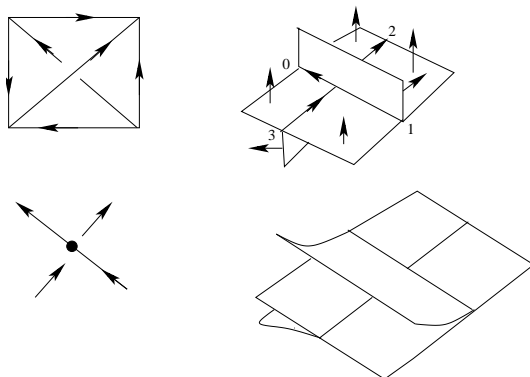

FIGURE 1.   From a branched tetrahedron to branched butterfly.

In every case, the branching encodes a structure of smooth *transversely oriented branched surface* on Σ embedded in the interior of M; hence Σ becomes a so called *branched standard spine* of M (see [12] for all details). This also justifies the name "branching". A branched butterfly associated to a branched tetrahedron is shown in Figure 1; the labels $0, 1, 2, 3$ refer to the order on the dual 2-faces of (Δ, b) determined by the branching (accordingly with the order of the opposite vertices); the decorated planar crossing on the left-bottom of the figure encodes all the other pictures.

- **Pre-branching:** A pre-branching ω on T is a system of orientations of the open 1-cells of $\mathrm{Sing}(\Sigma)$ such that at every quadrivalent vertex of $\mathrm{Sing}(\sigma)$ two branches are ingoing and two are outgoing. This can be equivalently rephrased in terms of a system of transverse orientations on the 2-faces of T.

Given a branched triangulation (T, b) or a pre-branched triangulation (T, ω) of $\hat{M}$ every *positive* naked move $T \to T'$ (ideal or not) can be enhaced to some decorated move $(T, b) \to (T', b')$ or $(T, \omega) \to (T', \omega')$. This means that in both cases the decorations coincide on the portion of triangulation which persists in both T and T'; such a decorated move is also called a b- or pb-*transit*. A negative decorated move is by definition the inverse of a positive one.

If M is *oriented*, every branching b induces a pre-branching ω_b, by taking the prevailing dual edge orientation as above; every b-move $b \to b'$ induces a pb-move $\omega_b \to \omega_{b'}$.

By using only ideal moves we define the *decorated ideal transit equivalences* with quotient sets denoted $\mathcal{B}^{id}(M)$ and $\mathcal{PB}^{id}(M)$ respectively. Similarly we define the *completed* decorated relations with quotient sets $\mathcal{B}(M)$ and $\mathcal{PB}(M)$. Pre-branchings are much more flexible than branchings and are the basic ingredient for the theory of *taut* triangulations [16]. In particular every naked ideal triangulation T carries pre-branchings while there are naked triangulations, even for oriented M, which does *not* carry any branching. On the other hand, every M admits branched ideal triangulations. Quantum hyperbolic state sums were originally supported by branched triangulations (of oriented manifolds); since [6] it is clear that pre-branching is definitely the most funtamental structure governing such state sums. Often pre-branchings (on oriented M) are encoded by auxiliary decorations called *weak-branchings* which reveal in a more trasparent way a geometric content. We will occasionally make use of them referring for the details to [5], [6] and also [8].

Branched connectivity results. Here is two main results of the paper, see Section 3.

Theorem 1.4. *For every M, $\mathcal{B}(M)$ consists of one point.*

Theorem 1.5. *For every M, $\mathcal{B}^{id}(M)$ consists of one point.*

A few comments are in order:
  (1) A somewhat demanding proof of Theorem 1.4 is given in [13], starting from Lemma 2.1, in terms of branched spines. We will provide an alternative quick proof in terms of triangulations, based again on Lemma 2.1 and the first two steps in the realization of the (naked) barycentric subdivision of a given ideal triangulation T by means of positive $2 \to 3$ and $1 \to 4$ moves (see [24] Section 2.5). A simple but important ingredient will be the elementary move of *inverting a good ambiguous edge* which can be added without modifying the b-ideal transit equivalence.
  (2) As for the naked ideal connectivity result in the strong version mentioned above, we will give a proof of Theorem 1.5 based on the validity of Theorem 1.4, by applying suitable branched versions of Matveev's *arch and associated constructions*. The underlying naked configurations which we actually apply these constructions to are considerably simpler that the general ones faced in the proof of the strong version of Theorem 1.3; also the branched enhancement will benefit from this simplification.

On the structure of $\mathcal{PB}^{id}$. In contrast with $\mathcal{B}^{id}(M)$, in general $\mathcal{PB}^{id}(M)$ is far to be trivial, even infinite. We will get some information about it, in particular we characterize the (one-point) image of $\mathcal{B}^{id}(M)$ in $\mathcal{PB}^{id}(M)$ via the correspondence $b \to \omega_b$, provided that M is oriented.

Restricted transits. Pre-branched and branched moves are naturally organized in subfamilies which give rise to restricted transit equivalences. In the branching setting, the so called ideal *sliding* transits had been widely studied since [12]. We shortly revisit these early results, with some complement, and outline a (partially conjectural) conceptually different approach to Theorem 1.5 and eventually also to Theorem 1.3. The basic idea is to point out some structures of differential topological nature on M which are carried by every branched ideal triangulation (T, b) of $\hat{M}$, are preserved by the sliding transits and can be modified by the full branched transits. Complements mainly concern the so called carried *horizontal foliation*. In the pre-branching setting, and assuming M oriented, the *non ambiguous* equivalence has been introduced in [5] and leads to interesting examples of so called *non*

ambiguous structures, also related to the theory of *taut* triangulations [16], with the associated *reduced* quantum hyperbolic invariants (see also [4]). The non ambiguos relation lifts to a specialization of the sliding one on branched triangulations; we point out a few specific insights into the branching theory, again in terms of carried structures preserved by the non ambiguous and which can be modified by the whole slidings transits. In [7] we have developed a 2D counterpart of the present paper. This theme also emerged in [5], Section 5 within a so called "holographic" approach to 3D non ambiguous structures.

2. Generalities on decorated triangulations and their transits

First let us recall the *ideal* naked moves. The $2 \leftrightarrow 3$ move is illustrated in Figure 2; let us forget the edge orientations to see the naked move; the arrows gives us also an instance of branched move (see below). The positive move applies at every couple of (abstract) tetrahedra with a common 2-face which are replaced by three tetrahedra around a new edge. Both triangulations share 6 triangular faces on the boundary of the triangulated region.
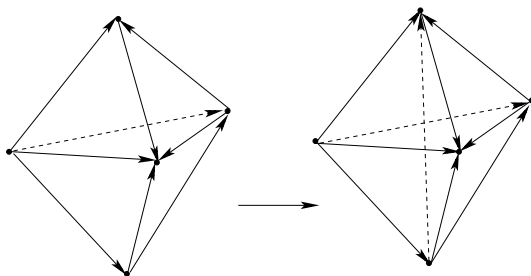
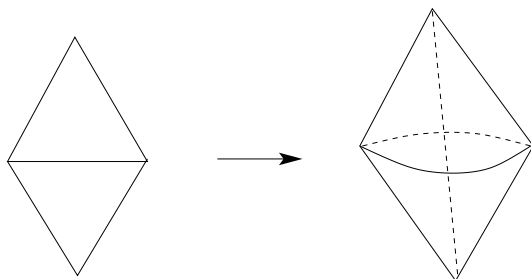

FIGURE 2.   The $2 \leftrightarrow 3$ move.

FIGURE 3.   The ideal quadrilater $0 \leftrightarrow 2$ move.

Figure 3 illustrates the naked *quadrilateral* $0 \leftrightarrow 2$ ideal move. The positive one applies at every quadrilateral made by two triangles with a common edge (a diagonal). It is replaced by a "pillow" triangulated by two tetrahedra glued along a quadrilateral which is a copy of the initial one on which a diagonal exhange has been performed. The boundary of the pillow is made by two copies of the initial quadrilateral glued along the common boundary.

In Figure 4 we show the two moves that generate (together with the above ideal ones) the *completed* transit relation. In fact we can eliminate one of them without modifying the relation (see also [24]). We will freely use both. The positive *triangular* $0 \to 2$ move applies at every triangle. It is repalced by a pillow triangulated by two tetrahedra glued along a copy of the initial triangle on which a 2D stellar $1 \to 3$ move has been performed. The boundary of the pillow is made by two copies of the initial triangle glued along the common boundary. The positive $1 \to 4$ move is shown on the bottom of Figure 4; in Figure 5 we see how it acts on a dual butterfly.
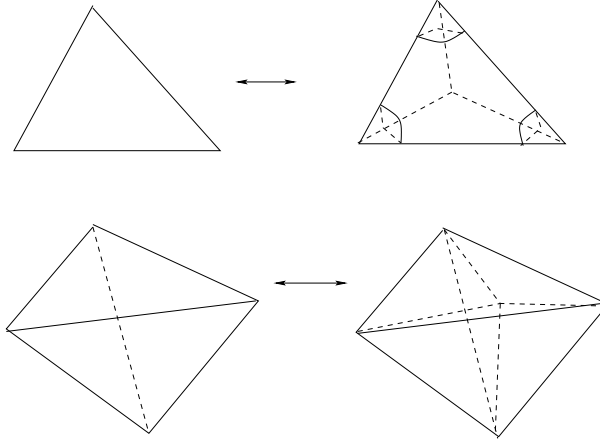
FIGURE 4.   The triangular $0 \leftrightarrow 2$ and the $1 \leftrightarrow 4$ moves generating the completed transit relation.
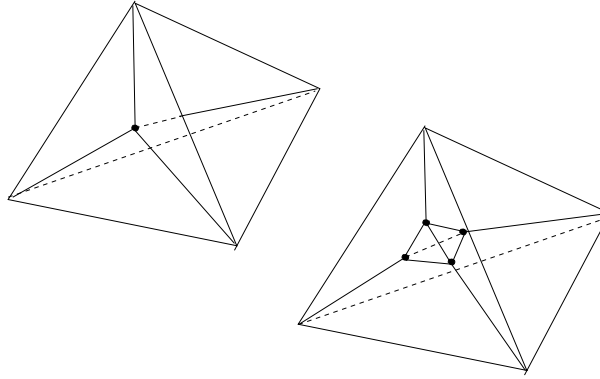

FIGURE 5.   A butterfly and its modification by a stellar $1 \to 4$ move.

Decorated transit. Let $T \to T'$ be a *positive* ideal naked move. We describe the decorated enhancements $(T, d) \to (T', d')$ where d, d' are either branchings or pre-branchings. Consider first a $2 \to 3$ move. Then T and T' share (on the portion involved in the move) 9 edges and 6 2-faces. If $d = b, d' = b'$ are branchings we require that b and b' agree at these persistent 9 edges. If $d = \omega, d' = \omega'$ are pre-branchings then we require that the transverse orientations agree at those 6 persistent 2-faces. If we consider a quadrilateral $0 \to 2$ move, in the branching case we require that the pillow boundary is made by two *branched* copies of the initial branched triangulated quadrilateral. Similarly in the case of pre-branchings we require that the transverse orientations at the pillow boundary are two copies of the transversal orientations at the triangles of the initial quadrilateral. A *negative d*-transit is by definition the inverse of a positive one.

If M is *oriented*, every branching b incorporates a pre-branching ω_b. If $b \to b'$ is a b-transit, then it induces a *pb*-transit $\omega_b \to \omega_{b'}$. It is easy to see that for every positive ideal transit $T \to T'$ and for every decoration (T, d) then we can enhace it to a d-transit $(T, d) \to (T, d')$ (see below for more details). On the other hand *there are decorations (T', d') such that the negative ideal move $T \leftarrow T'$ cannot be enhaced to any d-transit*. Moreover, this happens for (T', b') if and only if it happens for $(T', \omega_{b'})$. Hence there is a natural forgetting map

$$\phi : \mathcal{B}^{id}(M) \to \mathcal{P}\mathcal{B}^{id}(M), \ \phi([T, b]) = [(T, \omega_b)] \ .$$

For the further two moves generating the completed relation we do similarly.

Here is a first useful reduction in order to study the decorated transit equivalences. In fact next Lemma reduces the study to decorations carried by a same triangulation T.

Lemma 2.1. *For every M, for every triangulations (T_1, d_1) and (T_2, d_2) of $\hat{M}$, there are (T, d) and (T, d') such that (T_1, d_1) is equivalent to (T, d) and (T_2, d_2) is equivalent to (T, d').*

Proof. By [20], there are finite sequences of naked positive ideal moves $T_j \Rightarrow T$, $j = 1, 2$ (including both $2 \to 3$ and quadrilateral $0 \to 2$ moves). By positivity, there is no obstruction to enhance them to sequences of decorated transits.

$\square$

2.1. A combinatorial classification of decorated transits.

Definition 2.2. Given a *positive* ideal move $T \to T'$ and a decoration (T, d) we say that a d-transit $(T, d) \to (T', d')$ is *forced* if it is the unique enhancement of the naked move with the given initial decoration.

It is easy to see that if a decorated transit is not forced, then there are exactly two such enhancements. Let us fix some notations. A positive $2 \to 3$ move acts on the union of two "abstract" tetrahedra $\tau_1 \cup \tau_2$ which share one triangle t. We denote by $v_j \in \tau_j$ the vertex opposite to t. A naked positive quadrilateral $0 \to 2$ move acts on the union of two triangles $t_1 \cup t_2$ which share one edge e. We denote by $v_j \in t_j$ the vertex opposite to e.

Definition 2.3. A positive ideal b-transit $(T, b) \to (T', b')$ is called a *bump transit* if the vertices v_1 and v_2 (in (τ_j, b) or in (t_j, b) as above) are both either a pit or a source. A positive ideal b-transit $(T, b) \to (T', b')$ is called a *sliding transit* if it is not a bump transit. A negative b-transit is either bump or sliding if it is the inverse of a positive one.

We denote by $\mathcal{S}^{id}(M)$ the quotient set for the ideal s-transit relation generated by sliding b-transits. Hence we have a natural surjective projection

$$\mathcal{S}^{id}(M) \to \mathcal{B}^{id}(M) .$$

Now we recall the notion of *non ambiguous transit*; in doing it we stipulate that M is *oriented*.

Definition 2.4. (1) A positive ideal pb-transit $(T, \omega) \to (T', \omega')$ is *non ambiguous* if it is forced.
(2) A positive ideal b-transit $(T, b) \to (T', b')$ is *non ambiguous* if $(T, \omega_b) \to (T', \omega_{b'})$ is non ambiguous.
(3) A negative decorated transit is non ambiguous if it is the inverse of a non ambiguous positive one.

We stress that (2) is not the immediate definition of non ambiguous b-transit one would wonder. It is actually stronger. In fact we have (see below for more details):

- If $(T, b) \to (T, b')$ is non ambiguous, then it is forced.
- There are instances of forced $(T, b) \to (T', b')$ which are ambiguous.

The non ambiguous transits define restricted *na*-transit equivalences. We denote by $\mathcal{NA}^{id}(M)$ the corresponding quotient set in the case of pre-branchings; $\mathcal{BNA}^{id}(M)$ the one for branchings. We have a natural surjective projection

$$\mathcal{BNA}^{id}(M) \to \mathcal{S}^{id}(M) .$$

Non ambiguous ideal pb-transits are widely characterized and discussed in [5]. Now we make a more accurate analysis of the distributions of ideal b-transits in such sub-families. We have defined above the signs $*_{(\Delta, b)}$ when M is oriented. If M is not necessarily oriented (orientable) we can fix anyway a local auxiliary orientation on the (abstract) portion involved by a given move, and the signs $*_{(\Delta, b)}$ are defined as well. The initial configurations of a positive ideal $2 \to 3$ b-moves are in bijection with the total orderings of the 5 vertices of $\tau_1 \cup \tau_2$, hence they are 120. Every such an ordering induces a total ordering of the vertices of both τ_1 and τ_2 which are respectively encoded by means of the labels $\{0, 1, 2, 3\}$ and determines the branchings (τ_j, b). We can organize such configurations by 40 *types* which are classified by the couples

$$((*_1, a_1), (*_2, a_2)) \in (\{\pm 1\} \times \{0, 1, 2, 3\})^2$$

where $*_j$ is the b-sign of (τ_j, b), a_j is the order number of v_j with respect to the vertex ordering on τ_j. Each type carries 3 configurations which form the orbit of the group of cyclic permutations of the vertices of t. The (non)ambiguous/sliding/bump nature of a configuration only depends on its type; so the types are distributed according to this classification. Below we list 20 types arranged along a few rows; each type has an implicit *symmetric* one obtained by exchange the two entries of the couple. This corresponds to exchanging the role of v_1 and v_2. It is understood that symmetric types belongs to the same row. So we have:

- **Non ambiguous** $2 \to 3$ b-**transits.**

$$((-1,1),(-1,0)), \ ((+1,1),(+1,0)), \ ((+1,2),(+1,3)), \ ((-1,2),(-1,3))$$

$$((+1,2),(-1,0)), \ ((-1,3),(+1,1)), \ ((-1,2),(+1,0)), \ ((+1,3),(-1,1))$$

$$((+1,2),(+1,1)), \ ((-1,2),(-1,1)) \ .$$

The last two are characterized by the fact that all 5 tetrahedra occurring in the transit share the same sign ± 1 (the example shown in Figure 2 is of this kind); sometimes we call them *Schaeffer's* transits and they play a distinguished role in the study of quantum hyperbolic state sums (see [5], [6]).

- **Ambiguous sliding** $2 \to 3$ b-**transits.**

$$((-1,1),(+1,1)), \ ((+1,1),(-1,1)), \ ((+1,2),(-1,2)), \ ((-1,2),(+1,2))$$

$$((-1,3),(-1,0)), \ ((+1,3),(+1,0)) \ .$$

The last two are characterized by the fact that although they are ambiguous (at the level of the induced pre-branchings), they are forced; so they are called *forced ambiguous b-transits*.

- $2 \to 3$ **bump transits.**

$$((+1,0),(-1,0)), \ ((-1,0),(+1,0)), \ ((+1,3),(-1,3)) \ ((-1,3),(+1,3)) \ .$$

Note that row by row, there are pairs of cases just related by the inversion of the b-signs. This reflects geometric symmetries and instances in a pair basically have the same qualitative features. A very similar combinatorial classification (including the presence of forced ambiguous instances) holds for the quadrilateral $0 \to 2$ move.

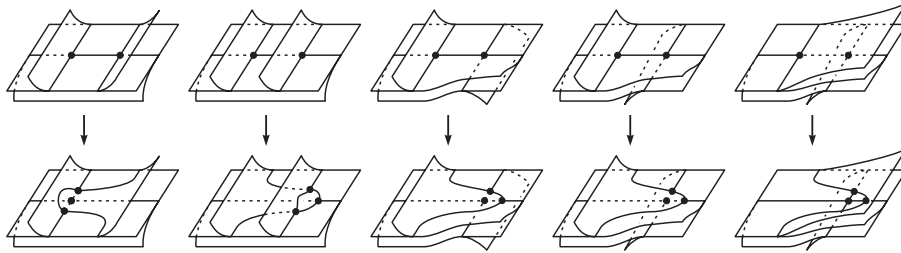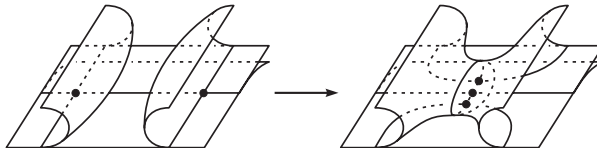FIGURE 6.   The sliding branched spine $2 \to 3$ move.

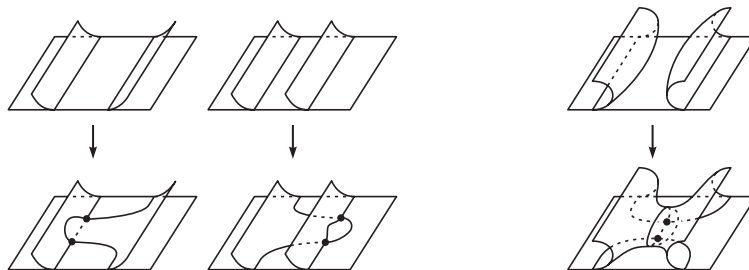FIGURE 7.   A branched spine $2 \to 3$ bump move.

FIGURE 8.   Branched lune moves.

Remark 2.5. In Figures 6, 7, 8 we see instances of the above classification "sliding vs bump" moves in terms of dual spines. A comment is in order. Every abstract tetrahedron and the dual butterfly have its own full group of symmetries. So a 'correct' picture of a naked moves should reflect them. For example in Figure 17 (B) in [24] we see such a symmetric picture of the $2 \to 3$ move in terms of spines. On the other hand, in Figure 18 of [24] we see another current picture of it; here the symmetry has been *broken* at both vertices of the initial spine and the moves becomes visually transparent: a region slides across a vertex to create two new ones. However this is somehow a visual artefact because such a symmetry break has no intrinsic meaning on a naked triangulation. Similarly in Figure 5 we show a symmetric picture of the $1 \to 4$ move in terms of spines, while in Figure 17 (A) of [24] we see a current non symmetric one. A branching can be also considered as a way to break the symmetry at every tretrahedron of a triangulation (see Figure 1) under a certain global coherence. We realize that sliding transits (in terms of dual branched spines) are realized by actual region sliding, while along a bump transit a region bumps into another one. We will return on this point in Section 6.

3. THE BRANCHED CONNECTIVITY RESULTS

Let (T, b) be an ideal branched triangulation of $\hat{M}$.

Definition 3.1. (1) An edge of T is said *ambiguous* if we can invert its orientation and keep a branched triangulation (T, b') (clearly the edge is ambiguous also in (T, b')).

(2) An ambiguous edge e of (T, b) is *good* if:

- (i) It does not support self-guing, that is it lifts to at most one edge in every abstract tetrahedron of T.
- (ii) Consider the branched star of e and its link $L(e)$ formed by the union of the opposite edge to e in each tetrahedron containing e. Then the branching does *not* make $L(e)$ an oriented circle.

We have

Lemma 3.2. *Let (T, b) and (T', b') differ by the inversion of one good ambiguous edge. Then they are ideally b-transit equivalent to each other.*

Proof. Let e be the good ambiguous edge which is inverted passing from b to b'. Then e must be ambiguous in every branched tetrahedron of its star. Notice that in a branched tetrahedron with ordered vertices v_0, v_1, v_2, v_3, the ambiguous edges are $v_0 v_1$, $v_1 v_2$, $v_2 v_3$. If the star consists of two tetrahedra, we recognize the final configuration of a positive ambiguous quadrilateral $0 \to 2$ b-transit. So we get the inversion of e by pre-composing this move with its negative inverse. If the star has more than two tetrahedra, by performing a positive $2 \to 3$ b-move at two tetrahedra in the star at which the two edges in $L(e)$ have conflicting orientations, e persists being good ambiguous and that number decreases by 1.

$\square$

Then we can add the elementary move of *inverting a good ambiguous edge* without modifying the ideal b-transit equivalence.

3.1. **Proof of Theorem 1.4.** Thanks to Lemma 2.1, it is enough to proof that for every ideal triangulation T, for every branchings b and b', $[T, b] = [T, b'] \in \mathcal{B}(M)$. We perform the first two steps of the construction of the (naked) barycentric subdivision of T by means of positive $2 \to 3$ and $1 \to 4$ moves (see [24], Section 2.5). First we apply the $1 \to 4$ move at every tetrahedron of T. We get a triangulation T_1 in which the 2-faces of T persist. Every such a face F is a common face of two tetrahedra of T_1; perform a further $1 \to 4$ move at one of them. Do it for every F getting a triangulation T_2. The faces F persit also in T_2. Every F is a common face of two tetrahedra of T_2. Perfom the $2 \to 3$ move that eliminate F. Do it for every F as above. We get our final triangulation $\tilde{T}$. Now let us enhance the composite transit $T \Rightarrow \tilde{T}$ to branched transits $(T, b) \Rightarrow (\tilde{T}, \tilde{b})$ and $(T, b') \Rightarrow (\tilde{T}, \tilde{b}')$ as follows: all branched $1 \to 4$ moves are such that the new vertex is a pit. The final $2 \to 3$ b-moves are bump moves and we stipulate that the new edges created by these moves are oriented in both $(\tilde{T}, \tilde{b})$ and $(\tilde{T}, \tilde{b}')$ in such a way that the vertices created by some $1 \to 4$ move keep the property of being a pit. The naked edges of T persist in $\tilde{T}$, and $\tilde{b}$ can differ from $\tilde{b}'$ only at some of these persistent edges. Finally we readily see that they are all good ambiguous in both $(\tilde{T}, \tilde{b})$ and $(\tilde{T}, \tilde{b}')$, hence we can pass from $\tilde{b}$ to $\tilde{b}'$ by inverting some of them.

$\square$

3.2. **Proof of Theorem 1.5.** Again by Lemma 2.1, it is enough to prove that for every ideal triangulation T of $\hat{M}$, for every branchings b and b', there is a composite ideal b-transit $(T, b) \Rightarrow (T, b')$. We start with the composite non ideal b-transit

$$(T, b) \Rightarrow (T_1, b_1) \Rightarrow (\tilde{T}, \tilde{b}) \Rightarrow (\tilde{T}, \tilde{b}') \Leftarrow (T_1, b_1') \Leftarrow (T, b')$$

constructed in the above proof. Now we want to apply branched versions of Matveev's *arch* and associated constructions to every $1 \to 4$ moves in order to eventually replace them in a systematic way with a composition of branched ideal moves. Naked arch and associated constructions are clearly discussed in [24], Section 5. By forgetting for a moment the branchings (so that the inversion of ambiguous edges becomes immaterial), our starting non ideal composite transits are much simpler than the general ones occurring in the proof of Theorem 1.4 in [24]. The main reason is that in our situation there are no interferences between the ideal and non ideal moves occurring in the given composite transit; then we can apply straightforwardly the naked construction described in Section 6 of [24] without any need of the subtle "moving the arch" procedure developed therein. Moreover we have the advantage of allowing the quadrilateral $0 \leftrightarrow 2$ move. So we can try to enhace such rather simple construction in the branched setting.
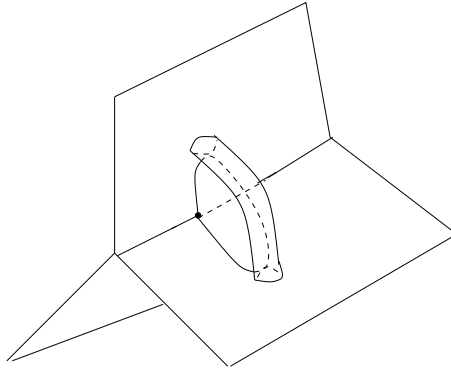
FIGURE 9.   Building an arch at an edge of a spine.

First let us decribe the arch construction associated to every naked $1 \to 4$ move $\mathcal{T}_1 \to \mathcal{T}_2$ producing a new material vertex v. One implements the following procedure. After the move there are six triangles t with common vertex v, so that the edge of t opposite to v belongs to $\mathcal{T}_1$. Select one t. Then select one, say e, of the two edges of t with vertex v; so in total there are 12 possible choices of the couple (t, e), each one called a *arch marking* (at the given naked $1 \to 4$ move). Every marking encodes

the location of an arch associated to the move. This is a quite localized construction that, roughly speaking, unglues the triangulation $\mathcal{T}_2$ at t an inserts one tetrahedron (with face/edge identifications) in such a way that the two vertices of e are eventually identified. It is easier to visualize an arch on the dual spine. The triangle t corresponds to a transverse spine edge. The arch opens a tunnel connecting the two boundary components of M corresponding to the vertices of e. In Figure 9 we show a realistic picture of it. Assume now that the move $(\mathcal{T}_1, \mathfrak{b}_1) \to (\mathcal{T}_2, \mathfrak{b}_2)$ is branched in such a way that v is a pit. We will deal only with this instance of branched non ideal move so we will understand it. The selected triangle t is now branched by $\mathfrak{b}_2$ and the edge e' of t opposite to v keeps the initial $\mathfrak{b}_1$-orientation. Then there are two possible choices for the edge e which are distinguished by the branching: either the $\mathfrak{b}_2$-orientation of e conflicts with the $\mathfrak{b}_1$-orientation of e' at the common vertex $e \cap e'$ or these orientations match; in this second case we say that $(e, \mathfrak{b}_2)$ carries the *prevailing orientation*. We have:

Claim 1. The naked arch encoded by the marking (t, e) can be enhaced to a branched arch (producing a branched triangulation $\mathcal{T}_2', \mathfrak{b}_2'$) which modifies only locally $(\mathcal{T}_2, \mathfrak{b}_2)$) if and only if $(e, \mathfrak{b}_2)$ carries the prevailing orientation. Hence there are in total 6 possible implementations of the branched arch construction associated to our branched $1 \to 4$ move.

Claim 2. The composition of a branched $1 \to 4$ move followed by the insertion of an associated branched arch can be undone (reobtaining the initial branched tertahedron (Δ, b) supporting the $1 \to 4$ move) by means of ideal b-moves localized on Δ.

First we complete the proof by assuming the Claims. Finally we will prove them.

A few remarks about our starting composite transit:

(1) Forgetting the branchings, the left and right composite transits are two copies of $T \Rightarrow T_1 \Rightarrow \tilde{T}$.
(2) On the left side, every edge which is present at some stage of the composite transit $(T, b) \Rightarrow (\tilde{T}, \tilde{b}')$ persits for ever keeping its branching orientation. The same fact holds on the right side composite transit $(\tilde{T}, \tilde{b}') \Leftarrow (T, b')$.

So every branched non ideal move $(\mathcal{T}_1, \mathfrak{b}_1) \to (\mathcal{T}_2, \mathfrak{b}_2)$ occurring on the left side has a twin move $(\mathcal{T}_2, \mathfrak{b}_2') \leftarrow (\mathcal{T}_1, \mathfrak{b}_1')$ on the right. Now we have to specify the (branched) arch marking at every $1 \to 4$ moves. For the move occurring in

$$(T_1, b_1) \Rightarrow (\tilde{T}, \tilde{b}) \Rightarrow (\tilde{T}, \tilde{b}') \Leftarrow (T_1, b_1')$$

we can choose two copies of the same (t, e) in every couple of twin moves, such that $(e, \mathfrak{b}_2) = (e, \mathfrak{b}_2')$, both carry the prevailing orientation, and e is not a persistent edge coming from T. For the couples of twin moves occurring in

$$(T, b) \Rightarrow (T_1, b_1), \ (T_1, b_1') \Leftarrow (T, b')$$

we take two copies of the same t and two copies of the same e (carrying the prevailing orientation) if the $\mathfrak{b}_1$ and $\mathfrak{b}_1'$ orientation agree on e'; otherwise the two branched arch markings differ by the choice of the edge e. Now one readily checks that no triangle occurring in a marking is destroyed by any ideal b-move of the composite transits. Then we can conclude by applying the above Claims, formally in the same way that works in the naked proof ([24]) Section 6) in the very favourable circumstance that "moving the marking" is never necessary. It remains to justify the Claims.

Claim 1: Again it is easier to deal in terms of dual spine. Possibly by using an auxiliary local orientation of M we can assume that the three involved portions of spine regions are oriented satisfying the branching condition. To build the arch we remove a small open 2-disk from two of them and we attach a copy of $S^1 \times [0, 1]$ glued to a monogon τ in such a way that $(S^1 \times [0, 1]) \cap \tau = \{p\} \times [0, 1]$. We need that the given region orientations propagate across $(S^1 \times [0, 1]) \setminus (\{p\} \times [0, 1])$ in such a way that the branching condition is kept; note that the monogon, that is its dual edge in $(\mathcal{T}_2', \mathfrak{b}_2')$, is ambiguous. It is now easy to check that this happens just when e carries the prevailing orientation. For completeness we describe also the corresponding one branched tetrahedron of $(\mathcal{T}_2', \mathfrak{b}_2')$ (with face/edge identification) inserted at the triangle t to build the arch. By adopting the notations stated above, let v_0, v_1, v_2 be the ordered vertices of $(t, \mathfrak{b}_2)$, so that $v = v_2$, $e = v_1 v_2$. Realize $(t, \mathfrak{b}_2)$ as the 2-face of an abstract branched tetrahedron $(\Delta, \mathcal{B})$ in such a way that its opposite vertex w is smaller that both

v_2 and v_1. Note that this requirement makes ambiguous the edge of Δ with vertices w and v_0. Now let us identify two 2-faces of $(\Delta, \mathcal{B})$ respecting the branching; precisely we identify $(t, \mathfrak{b}_2)$, that is the 2-face v_0, v_1, v_2, with the 2-face w, v_1, v_2, so that w and v_0 are identified at a same point p. Finally let us identify the edges pv_1 and pv_2, so that v_1 is identified with v_2.

□

Claim 2: It is enough to follow *backward* the sequence of spine moves given in Figure 9 of [3] (or equivalently the same sequence splitted in two parts accordingly to Figure 29 and 28 of [24]) by checking that it can be performed in the branched setting. Let us start with a branched butterfly as in Figure 10.
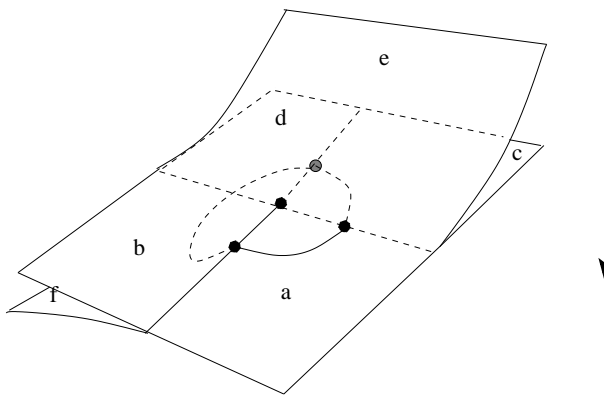

FIGURE 10.   A branched $1 \to 4$ move at a branched butterfly.

We assume that the transverse orientation at everyone of the 6 germs of region of the butterfly is given by the vertical vector pointing towards the bottom. In the picture these germs are labelled by a, b, c, d, e, f. Strictly speaking there should be a few such configurations to consider, also taking into account the (local) sign of the dual branched tetrahedron. We limit to discuss one as the other cases do not present substantial differences. The branched $1 \to 4$ move is obtained dually by attanching a 2-disk D along an embedded smooth circle into the smooth sheet of the butterfly made by the union of the regions labelled by a, c, f. This forms a bubble whose interior contains the new material vertex v. Moreover D is transversely oriented by a vertical vector pointing towards the top (accordingly to the fact that v is a pit in the branched triangulation). A branched $1 \to 4$ move, expressed in spine terms, is the composition of a branched bubble move followed by a positive branched $2 \to 3$ move. If we had built a (suitable) b-arch at the $1 \to 4$ move, this follows the inverse $3 \to 2$ move, so that we reach a configuration of b-arch at a branched bubble move as it is illustrated in Figure 11. The 2-disk D is now glued along a smooth circle embedded in the sheet made by the union of the regions labelled by a and c.

Now the disk D slides by means of a further branched $3 \to 2$ move realizing (by using the terminology of [24]) a *b-arch with membrane* as shown in Figure 12. The picture also shows the tranverse orientation of this membrane.

We can move by isotopy the membrane to reach the configuration of Figure 13. Now the transverse orientation of the membrane coincides with the one of the region labelled by e.

Now by means of a branched $2 \to 3$ move we reach the configuration illustrated in Figure 14.

14

14

By performing a further branched $2 \to 3$ move we reach the configuration illustrated in Figure 15. Finally this can be undone (getting the initial branched butterfly) by means of a negative sliding lune move. Both Claims, hence Theorem 1.5 are eventually achieved.

□
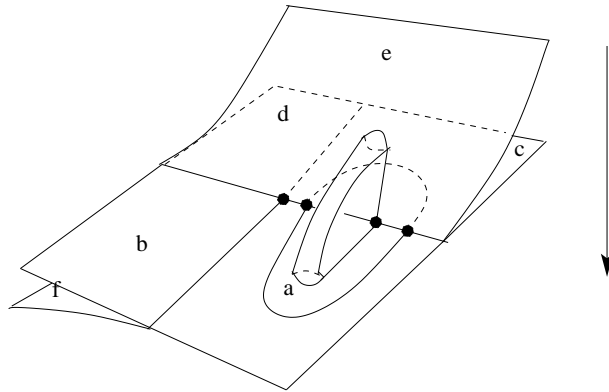
FIGURE 11.   A b-arch at a branched bubble move.
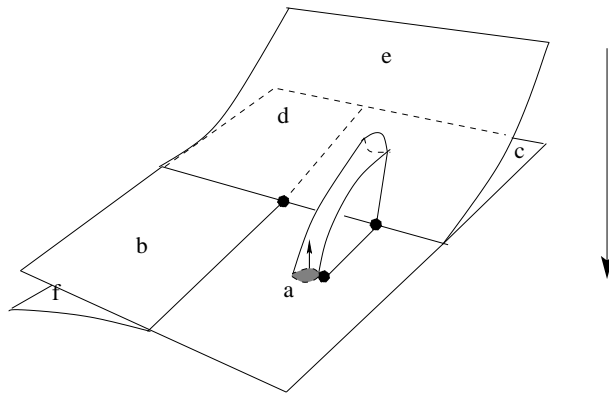
FIGURE 12.   A b-arch with membrane.
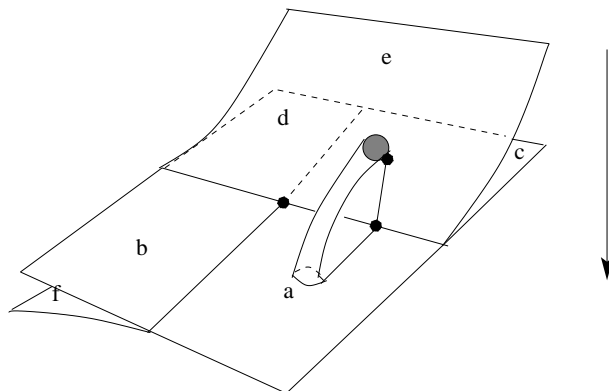
FIGURE 13.   A b-arch with membrane again.

4. ON $\mathcal{PB}^{id}(*)$

As for pre-branching we mainly refer to [5], accordingly with this reference in this section M is assumed *oriented*.

4.1. **Homological invariants.** Let T and Σ be as usual. Every pre-branching (T, ω) can be inter-preted as a *fundamental* cellular 1-$\mathbb{Z}$-cycle supported by the whole 1-skeleton $\mathrm{Sing}(\Sigma)$ of Σ. As a
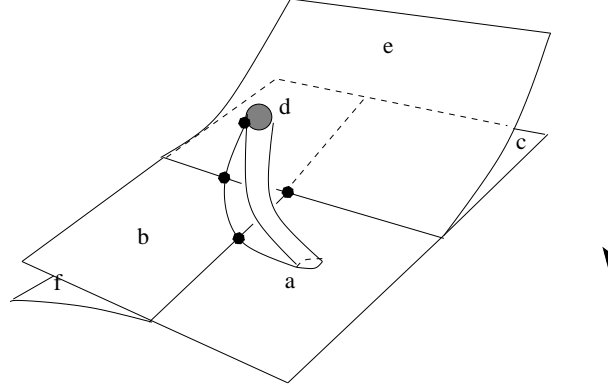
FIGURE 14.   Sliding the b-arch with membrane.
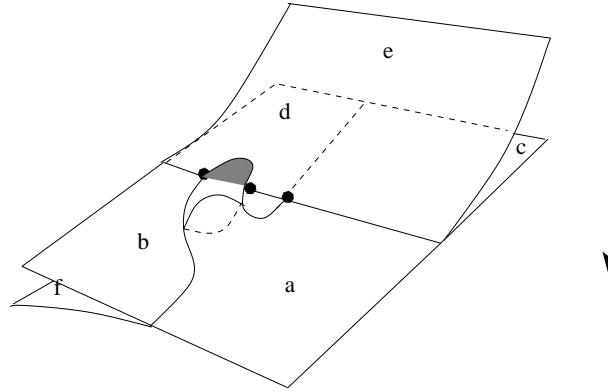
FIGURE 15.   A positive sliding lune move.

consequence of the "circulation lemma" of [15], a branching b can be interpreted as a *fundamental* cellular 2-$\mathbb{Z}$-chain supported by the whole 2-skeleton of Σ such that the boundary ∂b is a pre-branching (so that $\omega_b = \partial b$). Here "fundamental" means that all chain coefficients are equal to ± 1 (with respect to an arbitrary auxiliary system of orientations of the cells of Σ). Given a branching b, $\omega_b = \partial b$, we can take these orientations in such a way that all coefficients are equal to 1. We say that a cellular chain is *almost fundamental* if the coefficients belong to $\{0, \pm 1\}$. We have

Lemma 4.1. *For every pre-branching (T, ω),*
(1) The class $[\omega] \in H_1(M; \mathbb{Z})$ is invariant under ideal pb-transit equivalence.
(2) The reduction mod(2) $[\omega]_2 = 0 \in H_1(M; \mathbb{Z}/2\mathbb{Z})$.
(3) The class $[\omega]$ is even, i.e. $[\omega] = 2\alpha$ for some $\alpha \in H_1(M; \mathbb{Z})$.
(4) If $\omega = \omega_b$ for some branching b, then $[\omega] = 0$.

Proof. Point (1) follows immediately by looking at the local transits. Point (2) holds because (forgetting the orientation) ω is the boundary of the unique fundamental $\mathbb{Z}/2\mathbb{Z}$-2-chain on Σ. Point (4) has been remarked above. As for (3), it is a general fact that $[\omega]$ is even if and only if its reduction mod(2) $[\omega]_2 = 0 \in H_1(M; \mathbb{Z}/2\mathbb{Z})$. Let us give anyway a constructive proof in the spirit of transit equivalence. Assume that (T, ω) is such that T carries some branching b. Then $[\omega] - [\partial b] = [\omega] = [\omega - \partial b]$ and this last is a cycle of the form $z = 2a$, where a is an almost fundamental cycle. Then $[\omega] = 2[a]$. In general, in [12] Theorem 3.4.9 one finds an algorithm that for every naked triangulation T of M, produces a chain of positive $2 \to 3$ moves $T \Rightarrow T'$ such that T' carries some branching b. Enhace this to $(T, \omega) \Rightarrow (T', \omega')$. Then $[\omega] = [\omega']$ and the above argument applies to ω' and b.

$\square$

4.2. **Non triviality of $\mathcal{PB}^{id}(*)$.** By Theorem 1.5, the image of the forgetting map

$$\phi : \mathcal{B}^{id}(M) \to \mathcal{PB}^{id}(M)$$

consists of one point. Without using this result, we are going to see anyway that in general this image is a proper subset of $\mathcal{PB}^{id}(M)$. We will see later that $\mathcal{PB}^{id}(M)$ can be even infinite.

Lemma 4.2. $[(T,\omega)]$ *belongs to the image of* $\phi : \mathcal{B}^{id}(M) \to \mathcal{PB}^{id}(M)$ *if and only if there exists a branching* (T,b) *such that* $[(T,\omega)] = [(T,\omega_b)] \in \mathcal{PB}^{id}(M)$.

Proof. "If" is trivial. On the other hand, let $(T,\omega) \Rightarrow (T',\omega_{b'})$ a chain of pb-ideal moves such that (T',b') is branched. We can enhance the inverse naked chain $T \Leftarrow T'$ to a b-chain $(T,b) \Leftarrow (T',b')$; in fact there is not any stop because there is not at the pre-branching level. Finally $[(T,\omega)] = [(T,\omega_b)]$. $\square$

Remark 4.3. By the above proof we cannot conclude that $\omega = \omega_b$ (for some suitable implementation of $(T,b) \Leftarrow (T',b')$) because of the possible presence of forced ambiguous b-transit which might change the pre-branching at some step.

We know that a necessary condition in order that (T,ω) represents a point in $\mathrm{Im}(\phi)$ is that $[\omega] = 0 \in H_1(M;\mathbb{Z})$. In some case this is also sufficient; forthcoming examples will show that the hypothesis of next Lemma 4.4 is sharp.

Lemma 4.4. *Assume that* $H_2(M;\mathbb{Z}/2\mathbb{Z}) = 0$.
(1) Let (T,ω) *be a pre-branched triangulation of* $\hat{M}$ *such that* $[\omega] = 0 \in H_1(M;\mathbb{Z})$. *Then there exists a branching* (T,b) *such that* $\omega = \omega_b$.
(2) A triangulation (T,ω) *represents a point in* $\mathrm{Im}(\phi)$ *if and only if* $[\omega] = 0 \in H_1(M;\mathbb{Z})$.

Proof. Clearly $(1) \Rightarrow (2)$. As for (1), let

$$\omega = \partial\beta, \ \beta = \sum_{C \in \Sigma^{(2)}} \beta(C)C$$

where β is a cellular (not necessarily fundamental) $\mathbb{Z}$-2-chain on Σ. Consider the union of 2-cells such that $\beta(C)$ is even. This is a cellular $\mathbb{Z}/2\mathbb{Z}$-cycle of Σ. As Σ is a spine of M and $H_2(M;\mathbb{Z}/2\mathbb{Z}) = 0$, then this is necessarily empty. It follows that for every 2-cell C, $\beta(C)$ is odd. Define $b = \sum_C \dfrac{\beta(C)}{|\beta(C)|}C$.
This is a branching and $\partial b = \omega$. $\square$

In some case a branching is determined by the associated pre-branching.

Lemma 4.5. *Assume that* $H_2(M;\mathbb{Z}) = 0$. *Let* (T,b) *and* (T,b') *be branched triangulations of* $\hat{M}$ *such that* $\omega_b = \omega_{b'}$, *then* $b = b'$.

Proof. Let us orient the 1- and 2-cells of Σ by ω_b and b respectively, so that both ω_b and b considered as fundamental $\mathbb{Z}$-chains have all coefficients equal to 1. Set $\beta = b - b'$, $\partial\beta = \omega_b - \omega_b' = \alpha$. For every 2-cell C, $\beta(C) \in \{0,2\}$ as well as for every edge $e \subset \mathrm{Sing}(\Sigma)$, $\alpha(e) \in \{0,2\}$. Hence, $\partial\dfrac{\beta}{2} = \dfrac{\alpha}{2}$. As $\omega_b = \omega_{b'}$, then $\dfrac{\beta}{2}$ is an almost fundamental $\mathbb{Z}$-2-cycle which is empty because $H_2(M;\mathbb{Z}) = 0$. $\square$

Remark 4.6. The hypothesis of Lemma 4.5 is sharp. In fact, $H_2(M;\mathbb{Z})$ is free; if it is not zero, according to the above proof, there exists (T,b) such that b can be modified to some $b' = b - \partial 2z$, where z has coefficients in $\{0,\pm1\}$, $b \neq b'$, and $\omega_b = \omega_{b'}$ (see also the proof of Proposition 4.10).

Claim: *In general* $\mathrm{Im}(\phi)$ *is a proper subset of* $\mathcal{PB}^{id}(M)$.

Here is some examples; to treat them we use some notions introduced in [6], [5].
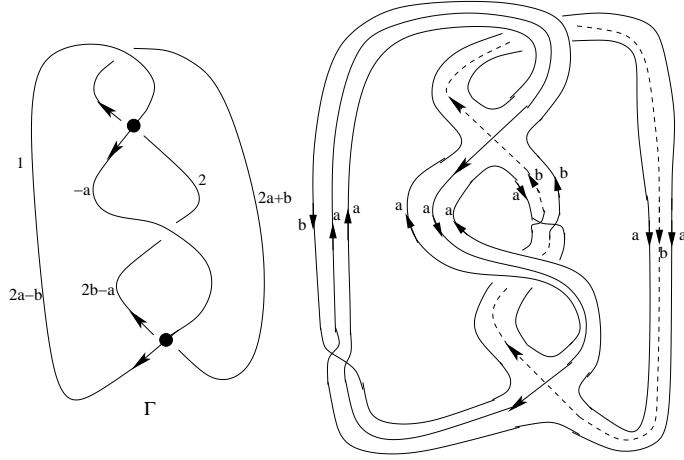
FIGURE 16.   No-brancheable, 1 .

(1) There are examples of naked ideal triangulations T of some $\hat{M}$ that do not carry any branching at all. It follows from Lemma 4.2 that every pre-branching (T, ω) does not represent a point in $\mathrm{Im}(\phi)$. Let us consider two concrete and instructive examples.

(a) Let T be the minimal triangulation by two tetrahedra of $\hat{M}$ where M is the "compact core" of the "figure-8-sister" cusped manifold. In Figure 16 we show a weakly branched realization $(T, \tilde{b})$ of it encoded by a $\mathcal{N}$-graph Γ (see [6], [5]). The "colors" $2, 1 \in \mathbb{Z}/3\mathbb{Z} \cong A_3$, $1 \leftrightarrow (0, 1, 2)$, the color 0 being omitted. The picture also shows a decoding of Γ, that is a regular neighbourhood of $\mathrm{Sing}(\Sigma)$ in the dual spine Σ. We use $\omega_{\tilde{b}}$ to orient $\mathrm{Sing}(\Sigma)$. Σ has two 2-regions on which we fix auxiliary orientations. The letters a and b refer to the coefficients of a cellular 2-chain β on Σ; they label the two oriented boundaries of the respective 2-regions. On the graph Γ we indicate the coefficients of $\partial\beta$. Then one computes immediately that $H_2(\Sigma; \mathbb{Z}/2\mathbb{Z}) \cong H_2(M; \mathbb{Z}/2\mathbb{Z}) = 0$; on the other hand, one realizes that for every $\mathbb{Z}$-2-chain β on Σ, $\partial\beta$ is not "fundamental", that is T does not carry any pre-branching ω such that $[\omega] = 0 \in H_1(M; \mathbb{Z})$.
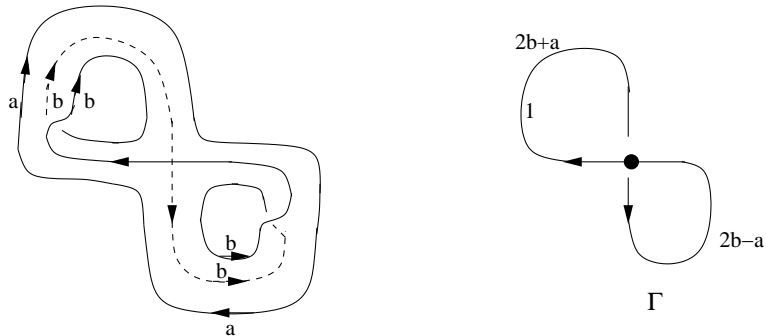
FIGURE 17.   No-brancheable, 2.

(b) Consider the weakly branched triangulation $(T, \tilde{b})$ (of some $\hat{M}$) encoded similarly to the above example in Figure 17. T consists of one tetrahedron, Σ has two 2-regions. By easy computations we see that $H_2(M; \mathbb{Z}) = 0$, $H_2(M; \mathbb{Z}/2\mathbb{Z}) \cong \mathbb{Z}/2\mathbb{Z}$. We realize also that every fundamental $\mathbb{Z}$-2-chain β on Σ is not a branching (that is $\partial\beta$ is not fundamental). On the other hand, the non fundamental chain β_0 such that $a = 1$, $b = 0$ is a non orientable branching. Hence, $\omega = \partial\beta_0$ is a pre-branching on T, such that $[\omega] = 0 \in H_1(M; \mathbb{Z})$ and nevertheless $[(T, \omega)]$ does not belong to $\mathrm{Im}(\phi)$. One can see

easily that ∂M consists of one spherical boundary component, so that $\hat{M}$ is a closed manifold (with a bit of effort one could realize that $\hat{M} = \mathbf{P}^3$ but this is not so important here).

(2) Let (T, ω) be a taut "layered" ideal triangulation of $\hat{M}$ where M is the compact core of a mapping torus T_ψ, having with fibre a punctured surface $S_V = S \setminus V$ of negative Euler characteristic. The boundary ∂M is made by tori. Such a (T, ω) is constructed by means of an ideal triangulation K of (S, V) (here the compact closed surface S plays the role of "$\hat{S}_V$") and of a sequence of naked flips $K \Rightarrow \psi(K)$, where ψ is an automorphism of S which pointwise fixes the punctures V (see [5] for the details). Then (T, ω) does not represent a point in $\mathrm{Im}(\phi)$. This follows from (1) of Lemma 4.1, because one can check that $[\omega]$ is a non zero multiple of the dual of the fibre. Fix any $2D$ branching $(K, \mathfrak{b})$. By a main result of [7], there is a sequence of b-flips $(K, \mathfrak{b}) \Rightarrow (\psi(K), \psi(\mathfrak{b}))$. By using the corresponding naked sequence we get an instance of layered taut (T, ω) as above; by using the b-sequence, we get a layered branched triangulation (T, b). These represent distinct points in $\mathcal{PB}^{id}(M)$.

The effects of the circuit move. Every pre-branching (T, ω) determines a natural decomposition of $\mathrm{Sing}(\Sigma)$ by *oriented circuits*. A *circuit move* on (T, ω) produces a new pre-branching (T, ω') by just inverting the orientation of one circuit. It is clear that every pre-branching carried by T can be obtained from any given (T, ω) by performing a finite sequence of circuit moves. Hence by adding these moves to the ideal pb-transits we generate an equivalence relation whose quotient set consists of one point (see [8, 6]). We have

Lemma 4.7. $\mathcal{PB}^{id}(M)$ *does not consist of one point if and only there are ideal pb-triangulations* (T, ω) *and* (T, ω') *of* $\hat{M}$ *which differ by a circuit move and represent different points in* $\mathcal{PB}^{id}(M)$.

Proof. Let (T_1, ω_1) and (T_2, ω_2) represent different points in $\mathcal{PB}^{id}(M)$. By Lemma 2.1, there are pb-transits $(T_1, \omega_1) \Rightarrow (T, \omega)$, $(T_2, \omega_2) \Rightarrow (T, \omega')$. (T, ω) and (T, ω') represent different points in $\mathcal{PB}^{id}(M)$ and are related to each other by circuit moves, hence at least one of them changes the class in $\mathcal{PB}^{id}(M)$.

$\square$

Proposition 4.8. *Let* (T, ω) *and* (T, ω') *be triangulations of* $\hat{M}$ *which differ by a circuit move supported by an oriented circuit* γ *in the* ω-*oriented* $\mathrm{Sing}(\Sigma)$. *Then:*
(i) If $2[\gamma] \neq 0 \in H_1(M; \mathbb{Z})$, *then* (T, ω) *and* (T, ω') *represent different points in* $\mathcal{PB}^{id}(M)$.
(ii) Forgetting the orientation, if $[\gamma]_2 \neq 0 \in H_1(M; \mathbb{Z}/2\mathbb{Z})$, *then* (T, ω) *and* (T, ω') *represent different points in* $\mathcal{PB}^{id}(M)$.
(iii) If either $H_1(M; \mathbb{Z}) \neq 0$ *and has no 2-torsion elements, or* $H_1(M; \mathbb{Z}/2\mathbb{Z}) \neq 0$, *then every ideal triangulation* T *of* $\hat{M}$ *carries two* (T, ω) *and* (T, ω') *which differ by a circuit move and represent different points in* $\mathcal{PB}^{id}(M)$.

Proof. (iii) is a consequence of either (i) or (ii). In fact fix any pre-branching (T, ω). The ω-oriented circuits of $\mathrm{Sing}(\Sigma)$ span both $H_1(M; \mathbb{Z})$ and $H_1(M; \mathbb{Z}/2\mathbb{Z})$. At least one, say γ, is such that either $2[\gamma] \neq 0$ or $[\gamma] \neq 0 \mod(2)$. Implement the circuit move at γ and get the required (T, ω').
(i) is a direct consequence of (2) of Lemma 4.1.
(ii) If $[\gamma]_2 \neq 0$, then $[\gamma] \neq 0$. If also $2[\gamma] \neq 0$, then we are as in point (i). The case when $2[\gamma] = 0$ is less evident. Lift the question in terms of weak branchings ([5], [6] , [8]). It is enough to detect a "character", say χ, of every weakly $(T, \tilde{b})$ which induces an invariant on $\mathcal{WB}^{id}(M) \sim \mathcal{PB}^{id}(M)$ and such that if $(T, \tilde{b})$ and $(T, \tilde{b}')$ differ by a circuit move along a circuit that verifies the conditions in the statement of (ii), then they have different χ. In [6] Remark 8.3 we already noticed that the *sign refined* QH state sums on QH-triangulations with non trivial c-weight provide instances of such characters.

$\square$

The sign refinement mentioned in the proof of (ii) above is a by-product of [8]. It would be interesting to produce such a character χ in a simpler way without referring to the whole demanding QH stuff. One would wonder that the union of the sufficient conditions in (i), (ii) of Proposition 4.8 is also necessary:

Question 4.9. Let (T, ω), (T, ω'), γ be as in the hypotheses of Proposition 4.8. Assume that they represent different points in $\mathcal{PB}^{id}(M)$. Does it hold true that $2[\gamma] \neq 0 \in H_1(M; \mathbb{Z})$ or $[\gamma]_2 \neq 0 \in H_1(M; \mathbb{Z}/2\mathbb{Z})$?

Finally let us show that $\mathcal{PB}^{id}(*)$ can be infinite.

Proposition 4.10. If $\operatorname{rank} H_1(M; \mathbb{Z}) \neq 0$, then $\mathcal{PB}^{id}(M)$ is infinite.

Proof. Assume that $\mathcal{PB}^{id}(M)$ is finite. Then there is a triangulation T of $\hat{M}$ such that every class in $\mathcal{PB}^{id}(M)$ can be represented by some (T, ω). By varying the pre-branching ω we get a finite subset $\Omega = \{[\omega]\} \subset H_1(M; \mathbb{Z})$. Take $\gamma \in H_1(M; \mathbb{Z})$ not belonging to Ω. There is a simple oriented curve C (not necessarily connected) traced on the dual spine Σ such that $\gamma = [C]$. By adding along every component C_i of C an annulus $A_i \subset \operatorname{Int}(M)$, we get a spine $\mathfrak{S} = \Sigma \cup_i A_i$ of M which is not even simple. We can thicken the boundary component of every A_i opposite to C_i to a solid torus to get a further (non simple) spine of M. By applying the "Bing house" trick at every solid torus we get a simple spine and possibly using some "lune move" we eventually get a standard spine Σ' of M such that the set of homology classes realized by the pre-branchings of Σ' contains $\Omega' = \{\alpha + 2\gamma | \ \alpha \in \Omega\}$. This is absurd.

$\square$

5. Structures carried by a branched ideal triangulation

Let $(M, \partial M)$, $\hat{M}$ be as usual. We are going to show that every branched ideal triangulation (T, b) of $\hat{M}$ carries a pair of transverse foliations of M; the 1-dimensional foliation will have oriented leaves, and this will be the case also for the 2-dimensional provided that M is oriented. Every such a foliation can be obtained by integration of some (integrable) fields of either tangent vectors or (possibly oriented) tangent 2-planes on M. We will say that two foliations are *homotopic* (*isotopic*) if they are obtained by integration of homotopic (isotopic) fields. In both cases one keeps fields integrability along isotopies. In the case of vector fields, integrability is preserved also along homotopies. This is not not required along homotopies of 2-planes fields.

5.1. The vertical foliation $\mathcal{V}_{T,b}$.

Definition 5.1. A *traversing foliation* $\mathcal{F}$ on M is a foliation by *oriented* 1-dimensional leaves which satisfies the following properties:

(1) Every leaf of $\mathcal{F}$ is a non degenerale closed interval which intersects transversely ∂M at its endpoints.

(2) There are *exceptional leaves* of $\mathcal{F}$ which are simply tangent to ∂M at a finite number of points. This tangency points form a compact (non necessarily connected) simple smooth *tangency line* $X = X_{\mathcal{F}}$ on ∂M. The smooth local model is

$$M = \{(x, y, t) \in \mathbb{R}^3 \ | t \leq y^2\}, \ \partial M = \{(x, y, t) \in \mathbb{R}^3 \ | t = y^2\}, \ X = \{t = y = 0\}$$

and $\mathcal{F}$ is given by the integration of the field $\dfrac{\partial}{\partial t}$ restricted to M.

(3) $\mathcal{F}$ is *generic* if every *generic* exceptional leaf is by definition tangent to the boundary at one point, and possibly there is a finite set of *non generic* exceptional leaves which are tangent at 2 points *with transverse tangency lines*: this means that they are transverse in ∂M provided that a neighbourd of one point is transported onto a neighbourhood of the other point by using the flow of the traversing foliation.

Since [12] we have pointed out (for oriented M and mainly in terms of *oriented* branched spines) that every ideal branched triangulation (T, b) of $\hat{M}$ carries a generic traversing foliation of M called here the *vertical foliations* $\mathcal{V} = \mathcal{V}_{T,b}$. In fact this holds as well if M is not orientable. We outlines its systematic construction in the form of a *puzzle*.

$\mathcal{V}$-**puzzle.** Let T be an ideal triangulation of $\hat{M}$. Associated to the family of abstract tetrahedra $\{\Delta\}$ which form T there is a family of *truncated tetrahedra* $\{\tilde{D}\}$. The boundary of every such a $\tilde{\Delta}$ has four triangular faces (corresponding to the four truncated vertices of Δ) and four hexagonal faces (the

truncation of the four 2-faces of Δ). The gluing in pairs of the abstract 2-faces of $\{\Delta\}$ which produces T restricts to a gluing in pairs of the hexagonal faces of $\{\tilde{D}\}$ which produces a cell decomposition $(\tilde{T}, \partial\tilde{T})$ of $(M, \partial M)$. The restriction $\partial\tilde{T}$ is in fact a triangulation of ∂M made by the triangular faces of $\{\tilde{D}\}$.

Recall now a classical way to prove that the Euler-Poincaré characteristic $\chi(Y)$ of a boundaryless compact manifold Y defined by means of the zero indices of any tangent vector fields on Y with isolated zeros coincides with its combinatorial definition in terms of any triangulation of Y (having only material vertices): given such a triangulation T we take its first barycentric subdivision $T^{(1)}$ endowed with a standard Δ-complex structure so that in particular every vertex of T is a pit. Then every symplex of $T^{(1)}$ (with ordered vertices) carries a so called *Whitney tangent vector field* which can be defined explicitly in terms of its barycentric coordinates (see [18]). All these locally defined vector fields match to define a globally defined vector field on Y with an isolated zero at each barycenter of the 'geometric' symplexes of T (with not necessarily ordered vertices) in such a way that the sum of these indices equals the combinatorial characteristic of T.
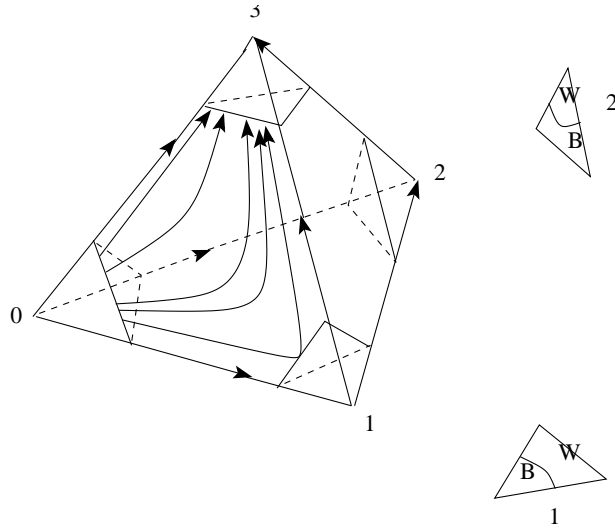

FIGURE 18.   Tiles for $(\mathcal{V}, \partial\mathcal{V})$.

From this general construction we retain that every branched tetrahedron (Δ, b) carries such a Whitney field which restricts to its 2-dimensional instance on every branched 2-face of (Δ, b) (see Figure 18 and also the top of Figure 21). Finally we consider the restriction of the oriented integral lines of these fields to every truncated tetrahedron $\tilde{\Delta}$. This gives us the tiles $(\tilde{\Delta}, \mathcal{V}_{\tilde{\Delta}})$ of our puzzle. For every branched triangulation (T, b) of $\hat{M}$, they match to produces the required vertical traversing foliation $\mathcal{V}_{T,b}$.

$\mathcal{V}$-boundary bicoloring. Every traversing foliation $\mathcal{F}$ of M, in particular a vertical foliation $\mathcal{V} = \mathcal{V}_{(T,b)}$, determines a *bicoloring*, denoted by $\partial\mathcal{F}$, of the components of $\partial M \setminus X_{\mathcal{F}}$: let us say that a component C is *white* (*black*) if the foliation is ingoing (outgoing) at C. For every tile $(\tilde{\Delta}, \mathcal{V}_{\tilde{\Delta}})$ denote by t_j, $j = 0, 1, 2, 3$, its triangular face at the truncated vertex v_j of (Δ, b) (as usual the vertices of (Δ, b) are ordered via a labelling by $0, 1, 2, 3$); then t_0 is all white, t_3 is all black; both t_1 and t_2 are divided by an arc of $X_{\mathcal{V}}$ into a white and a black portion; the white (black) zone of t_1 (t_2) contains two vertices of that triangular face (see again Figure 18). Denote by $W_b(\partial M)$ (resp. $B_b(\partial M)$) the union of the white (black) regions of ∂M determined by the boundary bicoloring $\partial\mathcal{V}$. Notice that

$$\chi(M) = \frac{1}{2}\chi(\partial M) = \chi(\overline{W_b(\partial M)}) = \chi(\overline{B_b(\partial M)}) \ .$$

M oriented. If M is *oriented* the colors can be encoded by an orientation: a black component keeps the boundary orientation (according to the usual rule "first the outgoing normal"), while a white component has the opposite orientation.

When M is oriented there is another systematic way to construct $\mathcal{V}$. Let M, (T, b), (Σ, b) be as usual. Let (Σ^*, b^*) be an "abstract" copy of the oriented branched surface (Σ, b), with its own branched smooth structure. Let us consider the oriented branched 3-manifold with boundary

$$F = F(T, b) = (\Sigma^* \times I, \hat{b}), \ I = [-1, 1] \ .$$

Its singular set is

$$\mathrm{Sing}(F) = \mathrm{Sing}(\Sigma^*) \times I$$

hence F has no "vertices", i.e. 0-dimensional singular strata. For every edge e of $\mathrm{Sing}(\Sigma^*)$, $\{e\} \times I$ is called a *switching surface* of F. For every vertex v of $\mathrm{Sing}(\Sigma^*)$, $\{v\} \times I$ is called a *pivot* of F. The orientation $\hat{b}$ on every 3-dimensional region of $F \setminus \mathrm{Sing}(F)$ is the product of the natural orientation of $I = [-1, 1]$ by the b^*-orientation of a 2-region of Σ^*. Note that we have inverted the factors order. Switching surfaces and pivots are oriented similarly. F carries the "vertical" foliation $\mathcal{V}^*$ by the oriented segments $\{x\} \times I$. Every pivot, swithching surface, or 3-dimensional region of F is union of leaves of $\mathcal{V}^*$. An interesting result of [15] is that M can be (piecewise linearly) embedded into F. By taking a suitable *normal smooth* embedding we can realize $\mathcal{V}_{T,b}$ as the restriction of $\mathcal{V}^*$ to M. This idea had been already exploited in [11]; we will add more precision about a systematic construction of such a normal embedding, again in the form of a puzzle. Before doing it, we summarize its main features.

Proposition 5.2. *For every branched triangulation (T, b) there is a normal smooth embedding $M \subset F(T, b)$ which satisfies the following properties:*

(1) *The restriction $\mathcal{V} = \mathcal{V}_{T,b}$ of the vertical foliation $\mathcal{V}^*$ of $F = F(T, b)$ is a generic traversing foliation of M which coincides with the one described via the $\mathcal{V}$-puzzle.*

(2) *Denote by M° the maximal subset of M formed by vertical segments which are leaves of both $\mathcal{V}^*$ and $\mathcal{V}$. Then M° includes $\mathrm{Sing}(F)$ and $F \setminus (\mathcal{N} \times I)$ where $\mathcal{N}$ is a regular neighbourhood $\mathcal{N}$ of $\mathrm{Sing}(\Sigma^*)$ in Σ^*.*

(3) *The vertical leaves contained in $\mathrm{Sing}(F)$ coincide with the exceptional leaves of $\mathcal{V}$. The pivots of F are the non generic exceptional leaves.*

(4) *The oriented branched surface $\Sigma \subset M \subset F$ is transverse to the leaves of $\mathcal{V}$, in such a way that:*

(i) *It intersects all leaves.*

(ii) *Every generic exceptional leaf intersects Σ at 2 points; every pivot intersects Σ at 4 points.*

(iii) *Every leaf which intersects $\mathrm{Sing}(\Sigma)$ is non exceptional and intersects Σ at one point.*

(iv) *The product orientation $I \times b$ coincides with $\hat{b}$.*

(5) *The normal embeddings of M in F are considered up to isotopy through normal embeddings, so that $\mathcal{V}$ is uniquely determined up to isotopy, preserving the exceptional leaves.*

$\square$

The normal embedding of M into $F(T, b)$ The construction below is illustrated in Figure 19.

(1) We decompose Σ^* (hence Σ) by "tiles" of three types: *butterfly*, "$Y \times J$", and *disk*. The butterflies form a branched regular neighbourhood of the vertices of Σ^*. Every butterfly has a boundary made by the union of four branched tripods and six simple arcs glued at eleven corners at which an arc and a tripod have a common endpoint. Every $Y \times J$ is the product of a branched tripod Y and a closed interval J. Its boundary is the union of two tripods and three simple arcs, with six corners. There is one such a tile at every edge of $\mathrm{Sing}(\Sigma^*)$. Butterflies and $Y \times J$ tiles glue at pairs of common boundary tripods to form a branched regular neighbourhood $\mathcal{N}$ of $\mathrm{Sing}(\Sigma^*)$ in Σ^*. The boundary $\partial \mathcal{N}$ is a union of smooth simple circles. The closure of every component of $\Sigma^* \setminus \mathcal{N}$ is a disk tile. The union of these disks intersect $\mathcal{N}$ along $\partial \mathcal{N}$.

(2) Let us generically denote by P such 2-dimensional tiles. Then $P \times I$ is the corresponding tile of $F = \Sigma^* \times I$. These 3-dimensional pieces match at the surfaces $\partial P \times I$ so that their union reconstructs
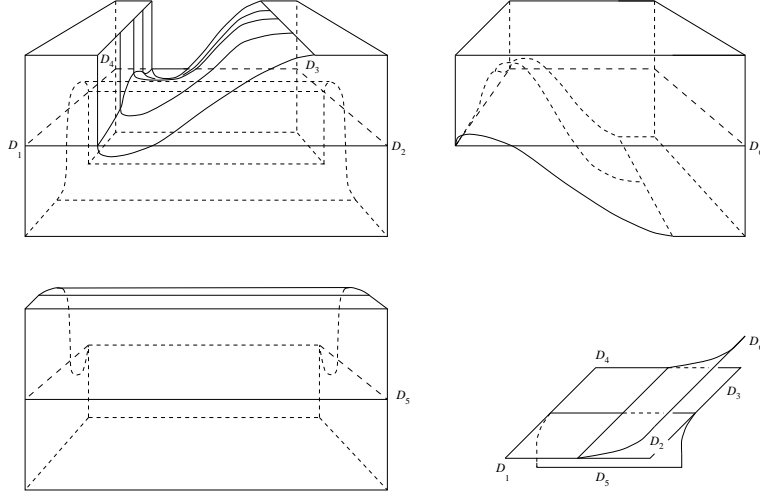
FIGURE 19.   Tiles for the normal embedding of M into $F(T, b)$.

the whole of F. Within every $P \times I$ we will specify a smoothly embedded 3-dimensional manifold Q_P (with boundary and corners), such that Q_P also embedds into M and the above matching coherently restricts to the surfaces $Q_P \cap (\partial P \times I)$; the union of the Q_P's eventually realizes the required embedding of M into F. We stress that every Q_P will be determined by the actual embedding of (a copy of) P into M, by using both the branching b and the orientation of M. Let us describe Q_P, type by type.

• Let P be a disk. Then Q_P coincides with the whole of $P \times I$. The embedding of Q_P in M is such that $P \times \{0, \}$ is the copy of P in Σ.

• Let P be a tile of type $Y \times J$. Then also Q_P is a product of the form $S_P \times J$, where $S_P \subset Y \times I$, and for every $s \in J$, $S_P \times \{s\} \subset Y \times \{s\} \times I$ fiberwise. Let us denote by l_-, l_+ the two legs of the oriented branched tripod Y which induce the prevalent orientation on the central vertex x_0. The order of the legs is determined by the b-orientation of of $\mathrm{Sing}(\Sigma^*)$ and the orientation of M. Let l_0 be the other leg. Let us subdivide $l_\pm$, by its midpoint $x_\pm$. Hence $l_\pm = l'_\pm \cup l''_\pm$, where $l'_\pm = [z_\pm, x_\pm]$ and $l''_\pm = [x_\pm, x_0]$ Set $y_\pm$ the midpoint of $l''_\pm$, w the one of $l_0 = [x_0, w] \cup [w, p]$. On $l_\pm \times I$ consider function $t = f_\pm(x)$ such that:

$f_\pm$ is smooth on $l_\pm \setminus \{x_0\}$;

$f_\pm(x) = \mp 1$, if $x \le x_\pm$;

f_+ (resp. f_-) is incresing (decreasing) on $[x_\pm, y_\pm]$, decreasing (increasing) on $[y_\pm, x_0]$;

$f_\pm(y_\pm) = \pm 1/4$;

$f_\pm(x_0) = 0$, and the graph of $f_\pm$ is simply tangent to the vertical segment $\{x_0\} \times I$ at the point $(x_0, 0)$.

Set
$$S_P^+ = \{(x, t)| \ t \ge f_+(x)\}, \ S_P^- = \{(x, t)| \ t \le f_-(x)\} \ .$$
Finally set

$$S_P = S_P^+ \cup S_P^- \cup (l_0 \times I) \ .$$

Note that the boundary of S_P contains a smooth line, γ say, formed by the union of the graphs of the functions $f_\pm$ which is simply tangent to $\{x_0\} \times I$; hence the surface $\gamma \times J$ is simply tangent to $\{x_0\} \times J \times I$ along $\{x_0\} \times J \times \{0\}$. The embedding of Q_P into M is such that the copy of P in Σ is subdivided by:

$P \cap \{(l'_\pm \times J) \times I\} = (l'_\pm \times J) \times \{0\}$;

$P \cap \{([w, p] \times J) \times I\} = ([w, p] \times J) \times \{0\}$;

$P \cap \{((S_P^\pm \cup [x_0, w]) \times J) \times I\}$ is "parallel" to $\{\gamma \cup ([x_0, w]) \times \{0\})\} \times J$ with switching curve given by $\{w\} \times J \times \{0\}$.

• Let P be a butterfly. We can normalize the picture so that P is formed by a *plate* $\mathcal{P}$ and two *wings* $\mathcal{W}_\pm$. The wings are ordered by the b-orientation of $\mathcal{P}$ and the orientation of M; within M it makes sense that $\mathcal{W}_+$ lies "over" $\mathcal{W}_-$. We can also assume that $\mathcal{P}$ is obtained by removing from a square $Q = J^2$ (with coordinate (x, y)) four disjoint sectors of open 2-disks centred at the corners of Q; the boundary of every sector intersects ∂Q at an arc properly embedded in Q which near ∂Q is made by two orhogonal small segments. The four tripods in ∂P have centers in the midpoints of the edges of Q, two legs contained in $\partial \mathcal{P}$ and a further leg contained in $\partial \mathcal{W}_\pm$. The union of the wings intersects $\mathcal{P}$ at the cross $\{xy = 0\}$ (which is included in $\mathrm{Sing}(\Sigma^*)$). The b-orientation of the cross determines two bands $\mathcal{B}_\pm$ of $\mathcal{P}$ "on the left" of either $\{x = 0\}$ or $\{y = 0\}$. These are ordered according to the fact that the wing $\mathcal{W}_\pm$ folds over $\mathcal{B}_\pm$ in $\Sigma \subset M$. To fix the idea, let us assume that P corresponds by duality to a tetrahedron of (T, b) such that the b-sign $*_b = +1$ (the other case can be treated similarly). Then $\mathcal{B}_+$ is bounded by $\{y = 0\}$, while $\mathcal{B}_-$ is bounded by $\{x = 0\}$. Take $\mathcal{P} \times I \subset F$. This also embedds into M. By adopting the above notations, we can "dig a groove" in $\mathcal{B}_+ \times I$ and realize an embedding of $(S_P^- \cup (l_0 \times I)) \times J$ into $\mathcal{P} \times I$ (hence in M), so that $\{y = 0\} \subset \mathcal{P}$ is the tangency line. Then we can glue a copy of $S_P^+ \times J$ along $\{y = 0\} \times [0, 1]$. We call this a *thick wing*. The resulting space Q_P^+ embedds in both F and M. Q_P^+ can be glued to suitable pieces Q_* constructed as above along two edges (possibly the same) of $\mathrm{Sing}(\Sigma^*)$. We can manage similarly (and independently) on $\mathcal{B}_-$, dig a groove to realize an embedding of $(S_P^+ \cup (l_0 \times I)) \times J$ and complete it by a thick wing $S_P^- \times J$ along $\{x = 0\} \times [-1, 0]$. This produces Q_P^-. For every $\mathcal{P}$ consider the *intersection* $Q_P' = Q_P^+ \cap Q_P^-$. These can be assembled with the 3-dimensional pieces of the other types to get a spaces M' which embedds in both F and M; $M \setminus M'$ consists of the union of disjoint small neighbourhoods of the vertices of Σ (each one corresponding to the portion of $\mathcal{P} \times I$ where the two grooves cross). In order to get the whole of M, we define the ultimate Q_P by modifing by isotopy the two grooves (and consequently the two thick wings) in such a way that Q_P coincides with Q_P' near the boundaries and the grooves do not cross. Precisely, the new groove digged in $\mathcal{B}_+ \times I$ has tangengy line on $\{y = 0\} \times [0, 1]$ which is the graph of a smooth non negative bell function $t = g_+(x)$ which is equal to 0 near the boundary, and $g_+(0) = 2/4$ is its maximum value. Similarly, the new groove digged in $\mathcal{B}_- \times I$ has tangengy line on $\{x = 0\} \times [-1, 0]$ which is the graph of a smooth non positive bell function $t = g_-(y)$ which is equal to 0 near the boundary, and $g_-(0) = -2/4$ is its minimum value. The grooves are isotopically either lifted up or lowered consequently. The embedding of a butterfly of Σ into such a Q_P agrees with the embedding described above near the boundary and can be naturally extended in the interior.

We have achieved the promised *normal smooth embedding* of M into $F(T, b)$. By construction a normal embedding preserves the orientation. By construction we know exactly the intersection of M° with the pieces Q_P of any type.

5.2. **The horizontal foliation** $\mathcal{H}_{T,b}$. Let $X = X_\mathcal{V} \subset \partial M$ be the system of tangency lines of a vertical foliation $\mathcal{V} = \mathcal{V}_{T,b}$ as above. We can thicken every component C of X to an annulus A_C in ∂M, foliated by parallel copies of C. This gives us a system of *sutures* on the boundary ∂M. Denote by $\mathcal{A}$ the union of these annuli. The horizontal foliation $\mathcal{H} = \mathcal{H}_{T,b}$ has the following main properties:

(1) $\mathcal{V}$ and $\mathcal{H}$ are transverse foliations.
(2) The closure of every component of $\partial M \setminus \mathcal{A}$ is a leaf of $\mathcal{H}$, while $\mathcal{H}$ is transverse to ∂M along $\mathcal{A}$ and induces on every A_C the prescribed foliation. This is called the boundary configuration $\partial \mathcal{H}$ of $\mathcal{H}$.
(3) $\mathcal{H}$ is uniquely determined up to homotopy keeping the boundary configurations up to isotopy.

If M is oriented, $\mathcal{H}$ is oriented as well in such a way that $\mathcal{V}$ intersects it everywhere with intersection number equal to 1. Also $\mathcal{H}$ can be produced by a puzzle.

$\mathcal{H}$-**puzzle.** Every truncated tetrahedron $\tilde{\Delta}$ associated to (Δ, b) carries a tile $(\tilde{\Delta}, \mathcal{H}_{\tilde{\Delta}})$. This is illustrated in Figure 20. The picture shows also the boundary configurations which is in agreement with the tiles of $\partial \mathcal{V}$ considered above (including the 2D branching $\partial \omega_b$ provided that M is oriented - let us forget it in general). In the triangles t_1 and t_2 we see the trace of $\mathcal{A}$ and the colored complementary
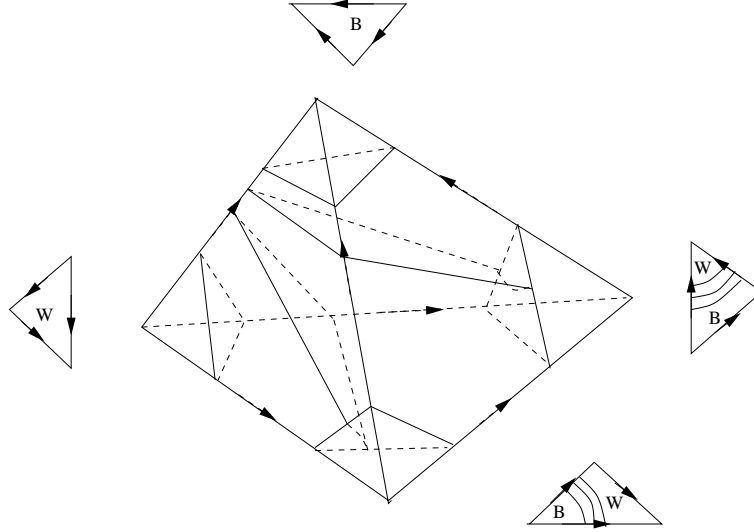
FIGURE 20. $3D$ tiles for $\mathcal{H}$.

portions. Every colored boundary piece is part of some horizontal leaf. In the bulk we see two typical leaves of $\mathcal{H}_{\tilde{\Delta}}$ which are transverse to ∂M along $\mathcal{A}$. The trace of $\mathcal{H}_{\tilde{\Delta}}$ on each hexagonal face of $\tilde{\Delta}$ is a tile of the $2D$ analogous of $\mathcal{H}_{\tilde{\Delta}}$ (see [7]). This is illustrated on the bottom of Figure 21.
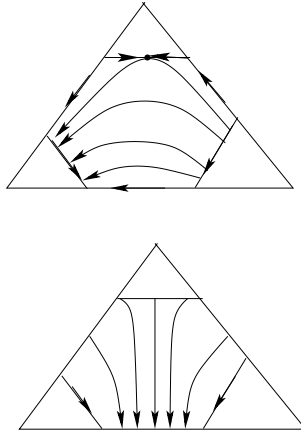

FIGURE 21. $2D$ tiles.

If M is oriented, also $\mathcal{H} = \mathcal{H}_{T,b}$ can be produced starting from a normal smooth embedding of M into $F = F(T,b)$. F carries also a horizontal foliation $\mathcal{H}^*$ with oriented branched leaves of the form $\Sigma^* \times \{t\}$. $\mathcal{H}$ is not immediately equal to the restriction $\mathcal{H}'$ of $\mathcal{H}^*$ to M. They coincide on M°, but $\mathcal{H}'$ has a somewhat complicated behaviour at ∂M on $M \setminus M^\circ$. Eventually $\mathcal{H}$ is homotopic to $\mathcal{H}'$.

6. On $\mathcal{S}^{id}(*)$

Now we can understand the meaning of the combinatorial classification of ideal b-transit (see Section 2.1). We mainly refer to [10] [12]. We have

Proposition 6.1. *Let $(T,b) \to (T',b')$ be an ideal ($2 \leftrightarrow 3$ or quadrilateral $0 \leftrightarrow 2$) branched transit. Then the following facts are equivalent to each other:*

(1) It is a sliding transit;

(2) $\partial \mathcal{V}_{(T,b)} = \partial \mathcal{V}_{(T',b')}$, that is the boundary bicoloring of the vertical foliations is preserved (up to isotopy);

(3) There is a smooth isotopy $\Psi : M \times [0,1] \to M$, $\psi_t = \Psi_{|M \times \{t\}}$, such that:

(i) $\psi_0 = id$; for every $t > 0$, ψ_t is an embedding onto $M_t \subset \text{Int}(M)$ and $M \setminus M_t$ is a collar of ∂M.

(ii) For every t, the restriction of $\mathcal{V}_{(T,b)}$ to M_t is a traversing foliation $\mathcal{F}_t$ which is not generic at one value $t_0 \in (0,1)$; hence the pullback $\mathcal{V}_t := \phi_t^*(\mathcal{F}_t)$ is a traversing foliation on M.

(iii) For every $t \in [0, t_0)$, $\mathcal{V}_t$ is isotopic to $\mathcal{V}_{(T,b)}$; for every $t \in (t_0, 1]$, $\mathcal{V}_t$ is isotopic to $\mathcal{V}_{(T',b')}$

In particular $\mathcal{V}_t$ is a homotopy through traversing foliations that connects $\mathcal{V}_{(T,b)} = \mathcal{V}_0$ with $\mathcal{V}_{(T',b')}$.

Then implications "(3) $\Rightarrow$ (2)" holds in general for every homotopy through traversing foliations: such a homotopy induces an isotopy of the boundary bicolorings (see [12], Lemma 4.3.8). In such a generality "(2) $\Rightarrow$ (3)" fails, but it is true in the restrictive hypothesis of the Proposition. This can be checked move by move; see again [12].

Point (a) of the following Proposition is equivalent to Proposition 6.1 (2); point (b) adds information about the way the boundary bicoloring changes. For a proof see [12], Proposition 3.5.1.

Proposition 6.2. Let $(T,b) \to (T',b')$ be an ideal branched transit. Then:
(a) the following facts are equivalent to each other:

(1) It is a bump transit;

(2) $\partial \mathcal{V}_{(T,b)} \neq \partial \mathcal{V}_{(T',b')}$

(b) Precisely the bicolorings differ to each other by an instance of the following modifications:

(i) $\overline{B_{b'}(\partial M)}$ is obtained by adding to $\overline{B_b(\partial M)}$ one 1-handle embedded in $\overline{W_b(\partial M)}$ and one 2-disk embedded in $W_b(\partial M)$, disjoint from the attached handle;

(ii) The inverse of the modification in (i);

(iii) The modifications obtained as above provided that the roles of the white/black portions of ∂M are exchanged.

Remark 6.3. The above bicoloring modifications preserve the necessary property that
$$\chi(\overline{W_b(\partial M)}) = \chi(\overline{B_b(\partial M)}) \ .$$
We are ready to point out the intrinsic content of $\mathcal{S}^{id}(M)$.

Proposition 6.4. Let (T,b) and (T',b') be ideal branched triangulations of $\hat{M}$. Then:
The following facts are equivalent to each other:
(1) They represent the same point in $\mathcal{S}^{id}(M)$;

(2) $\mathcal{V} = \mathcal{V}_{(T,b)}$ and $\mathcal{V}' = \mathcal{V}_{(T',b')}$ are homotopic through traversing foliations.

"(1) $\Rightarrow$ (3)" by Proposition 6.1. Clearly "(3) $\Rightarrow$ (2)". The proof of "(2) $\Rightarrow$ (3)" is essentially equivalent to the proof of Theorem 4.3.3. of [12], see especially Proposition 4.4.9. There one considers closed oriented M with triangulations with only one vertex, but the proof runs in general without substantial differences. It deals in terms of the dual branched spines which at present are transversely oriented, not necessarily oriented. Actually the proof in easier here because we are allowing arbitrary sliding lune moves, so that we can avoid most of the discussion of Section 4.5. of [12]. Let us recall a few points of the proof: by trasversality, we can assume that the homotopy is *generic*; this means that every $\mathcal{V}_t$ is generic with the exception of a finite number of points $t_j \in (0,1)$, $j = 0, \ldots, n$ where the genericity can be lost according to a determined finite set of configurations. The boundary bicoloring is constant along the whole homotopy; for every generic $\mathcal{V}_t$ the traversing foliation is carried by transversely oriented branched *simple* spine Σ_t, such that $\Sigma_0 = \Sigma$, $\Sigma_1 = \Sigma'$ (hence they are standard); along every interval (t_j, t_{j+1}), the foliations as well as the spines are isotopic to each other, and by analyzing the possible configurations, one realizes that passing through every special value t_j has the effect to perform locally a sliding move (which makes sense also for simple, not necessarily standard, spines). It might actually happen that the standard setting is lost at some event where a negative

lune move is performed; however by using other sliding moves (modifying the homotopy itself) we can overcome it restoring the standard setting everywhere.

$\square$

Let us say that a homotopy as in (3) of Proposition 6.4 *realizes the sliding equivalence.*

Corollary 6.5. *If (T, b) and (T', b') represent the same point in $\mathcal{S}^{id}(M)$, a homotopy that realizes the sliding equivalence can be augmented to a homotopy of couples of trasverse foliations $(\mathcal{V}_t, \mathcal{H}_t)$ which induces an isotopy of the couples of boundary structures $(\partial \mathcal{V}_t, \partial \mathcal{H}_t)$, that is it connects the patterns of structures carried by (T, b) and (T', b') respectively.*

We can strengthen the intrinsic content of the sliding equivalence by considering more general 1-foliations on M. Let $\mathcal{F}$ be a non singular foliation on M by oriented curves which along the boundary ∂M has the same qualitative features of a traversing foliation but it is not necessarily a traversing foliation. Denote by $\partial \mathcal{F}$ its boundary configuration, that is the usual bicoloring. Call *admissible* every boundary configuration $\mathfrak{f}$ obtained in this way. We have (see [10]):

Lemma 6.6. *A boundary configuration $\mathfrak{f}$ is admissible if and only if $\chi(M) = \chi(\overline{W(\mathfrak{f})}) = \chi(\overline{B(\mathfrak{f})})$.*

Fix such an admissible boundary configuration $\mathfrak{f}$. Denote by $\mathcal{F}(M, \mathfrak{f})$ the set of non singular foliations $\mathcal{F}$ on M such that $\partial \mathcal{F} = \mathfrak{f}$ (up to isotopy), considered up to homotopy through non singular foliations which is an isotopy at ∂M. We stress that we are not requiring that $\mathcal{F}$ is traversing.

Let M' be obtained by removing an open 3-ball from M, creating a new spherical boundary component S. Given $\mathfrak{f}$ as above, denote by $\mathfrak{f}'$ the admissible boundary configuration at $\partial M'$ that extends $\mathfrak{f}$ in such a way that the bicoloring on S consists of one black and one white disk separated by one simple curve. Denote by $\mathcal{S}^{id}(M', \mathfrak{f}')$ the subset of $\mathcal{S}^{id}(M')$ formed by the classes of triangulations (T, b) of $\hat{M}'$ such that $\partial \mathcal{V}_{(T,b)} = \mathfrak{f}'$. Then, up to homotopy, the traversing foliation $\mathcal{V}_{T,b}$ is the restriction of some non singular foliation representing an element of $\mathcal{F}(M, \mathfrak{f})$. Hence there is a well defined map

$$\psi : \mathcal{S}^{id}(M', \mathfrak{f}') \to \mathcal{F}(M, \mathfrak{f}) \ .$$

A main result of [10] can be rephrased as follows.

Proposition 6.7. *For every admissible boundary configuration $\mathfrak{f}$ at ∂M, the map*

$$\psi : \mathcal{S}^{id}(M', \mathfrak{f}') \to \mathcal{F}(M, \mathfrak{f})$$

is bijective.

The particular case when M' is oriented and $\partial M'$ consists of just one spherical boundary component S had been early considered in [12]. In this case M is a closed manifold and $\mathcal{F}(M, \emptyset)$ is the set of arbitrary non singular foliations of M by oriented curves, considered up to homotopy sometimes called "combings"; the generalization in [10] (again for oriented M) is not hard. He we consider also M non orientable but the proof holds as well. First one proves at the same time that $\mathcal{S}^{id}(M', \mathfrak{f}')$ is non empty and the map ψ is onto (see Proposition 5.1.1 of [8]). The proof is based on Ishii's notion of *flow spines* [19]. For the injectivity of the map, see Theorem 5.2.1 of [8]. The basic idea is to 'cover' any homotopy with a chain of flow-spines connecting (T, b) with (T', b') such that the traversing foliation associated to one is homotopic through traversing foliations to the traversing foliations of the subsequent.

6.1. **An alternative approach to the connectivity results.** By using the above results, the natural projection $\mathcal{S}^{id}(M) \to \mathcal{B}^{id}(M)$ and the fact that $\mathcal{B}^{id}(M)$ consists of one point by Theorem 1.5, can be rephrased by saying that the bump moves modify in a transitive way the traversing foliations carried by the ideal branched triangulations of $\hat{M}$. By elaborating on this remark, we will outline a (partially conjectural) different, perhaps more conceptual approach to a proof of the main branched connectivity result and ultimately also of the naked one. With the notations of Proposition 6.7, let us fix an admissible boundary configurations $\mathfrak{f}$ and $\mathfrak{f}'$ of M and M'. We have

Proposition 6.8. *Let (T, b) and (T', b') be branched ideal triangulations of $\hat{M}'$ representing two different points of $\mathcal{S}^{id}(M', \mathfrak{f}')$. Then there is a composite ideal b-transit $(T, b) \Rightarrow (T', b')$ (necessarily including bump moves).*

Obviously this follows from Theorem 1.5 but we can prove it independently. $\mathcal{S}^{id}(M', \mathfrak{f}') \sim \mathcal{F}(M, \mathfrak{f})$ is an affine space on $H_1(M; \mathbb{Z})$ (hence they are in general infinite sets). Two non singular foliations on M with the same boundary configuration differs to each other (up to homotopy through foliations of the same type) by a so called *Pontrjagin move*; this can be realized by a so called *combinatorial Pontrjagin move* on (T, b) which is realized by a composite ideal b-transit as in the statement of the Proposition; details can be found in the proof of Proposition 6.3.1 of [12].

Proposition 6.9. *Let (T_1, b_1) be an ideal branched triangulations of $\hat{M}'$ representing a point of $\mathcal{S}^{id}(M', \mathfrak{f}'_1)$ and $\mathfrak{f}_2$ be another admissible boundary configuration for M. Then there is a composite ideal b-transit $(T_1, b_1) \Rightarrow (T_2, b_2)$ such that (T_2, b_2) represents a point in $\mathcal{S}^{id}(M', \mathfrak{f}'_2)$.*

Again it is a consequence of Theorem 1.5. However the statement is apparently weaker. Essentially we just require that the bump moves modify in a transitive way the admissible boundary configurations $\mathfrak{f}'$. Then we can make the following informal conjecture

Conjecture 6.10. *There is a substantially simpler proof of Proposition 6.9.*

Note that by using Proposition 6.2 (b), we can generate a 2D equivalence relation on the boundary configurations $\mathfrak{f}'$; so a preliminary task would be to get a 'simple' proof that these configurations are 2D equivalent to each other.

Assuming a (as much as possible) satisfactory solution of the conjecture, it is clear how to prove Theorem 1.5. Given two branched ideal triangulations (T_1, b_1) and (T_2, b_2) of $\hat{M}$ with boundary configurations $\mathfrak{f}_1$ and $\mathfrak{f}_2$, we perform on both a positive branched triangular $0 \to 2$ move (i.e. a bubble move in terms of dual spines) to get (T'_1, b'_1) and (T'_2, b'_2) representing points in $\mathcal{S}^{id}(M', \mathfrak{f}'_1)$ and $\mathcal{S}^{id}(M', \mathfrak{f}'_2)$ respectively. By Proposition 6.9 there is a composite ideal b-transit $(T'_1, b'_1) \Rightarrow (\tilde{T}_1, \tilde{b}_1)$ where this last represents a point in $\mathcal{S}^{id}(M', \mathfrak{f}'_2)$. Then by using Proposition 6.8 we get a composite ideal b-transit $(\tilde{T}_1, \tilde{b}_1) \Rightarrow (T'_2, b'_2)$. This is already an alternative proof of Theorem 1.4. Now to get Theorem 1.5 we have just to apply the arch and related constructions to undo the bubble moves.

Finally, given any naked ideal triangulation T of $\hat{M}$ (as we know it happens that it does not carry any branching), by theorem 3.4.9 of [12] there is a composite naked transit $T \Rightarrow T'$ (entirely composed by positive $2 \to 3$ moves) such that T' carries a branching. So a proof of the naked ideal connectivity results would be derived from the branched one.

7. On $\mathcal{NAB}^{id}(*)$

In this section we assume that the 3-manifold M is oriented. The non ambiguous transit equivalence of pre-branched ideal triangulations (T, ω) of $\hat{M}$ has been widely studied in [5]. An important remark is that every pre-branching determines a branching $\partial\omega$ on $\partial\tilde{T}$ (with the notations of Section 5.1). This is illustrated in Figure 22. The picture shows:

(1) A pre-branched tetrahedron (Δ, ω) and a branched (Δ, b) such that $\omega = \omega_b$.
(2) The four branched triangles in $(\partial\bar{\Delta}, \omega)$ (we stress again that they only depend on the pre-branching ω).
(3) The bicoloring of t_1 and t_2 determined by $\mathcal{V}(\bar{\tau}, b)$. By specifying the branching of t_j by labelling the vertices by $\{0, 1, 2\}$ as usual, we see the black portion of t_1 contains only v_0, while the one of t_2 contains both v_0 and v_1; v_2 is always in the white portion. This qualitative behavior does not depend on the choice of (Δ, b) such that $\omega = \omega_b$, in particular on the sign $*_b$ (equal to 1 in the picture).

The 2D version of the sliding equivalence of branched triangulations of surfaces can be developed as well. A main invariant of 3D non ambiguous classes of pre-branchings is the sliding equivalence class of $(\partial\tilde{T}, \partial\omega)$, hence ultimately the associated pair of oriented vertical and horizontal transvese foliations (with isolated singularities) on $\partial\tilde{T}$. In fact we are considering here the branched triangulations of surfaces all together, with arbitrary number of vertices, under both sliding diagonal exchanges and $1 \to 3$ stellar moves (see [5] and [7]).

If (T, b) is branched, we can apply the above constructions to the induced pre-branching ω_b. Firstly we note that the curve $X_\mathcal{V}$ of tangency lines of the vertical foliation $\mathcal{V} = \mathcal{V}_{T,b}$ is smoothly embedded
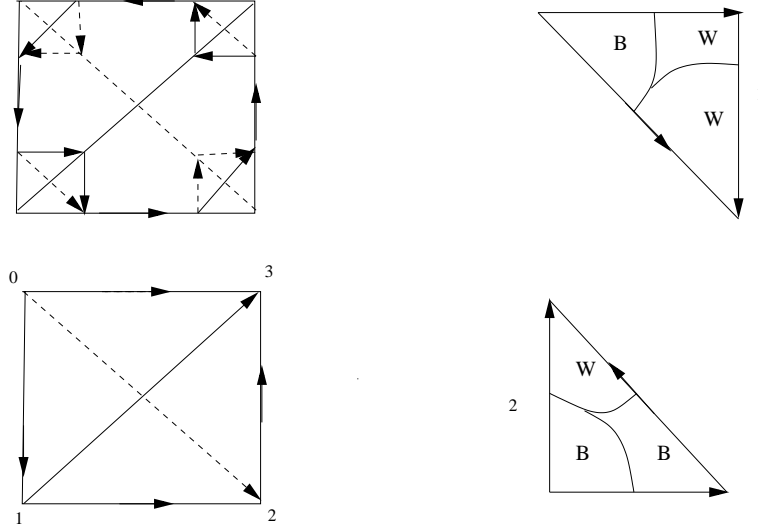
FIGURE 22. Tiles for $(\mathcal{V}, \partial\mathcal{V})$.

into the oriented train track θ_b in ∂M dual to $(\partial\tilde{T}, \partial\omega_b)$. The vertical foliations on $(\partial\tilde{T}, \partial\omega_b)$ can be recovered by means of the horizontal foliation $\mathcal{H} = \mathcal{H}_{T,b}$ of $(M, \partial M)$. We outline this construction.

(The "maws") Consider (T, b), (Σ, b), (Σ^*, b^*) as in Section 5.1.

(1) We define a branched singular foliation μ on (Σ^*, b^*) (hence on (Σ, b)). First we define μ along a branched regular neighbourhood $\mathcal{N}$ of $\mathrm{Sing}(\Sigma^*)$ in Σ^*, in such a way that:

- It is traversing $\mathcal{N}$;
- It is transverse to $\mathrm{Sing}(\Sigma^*)$ and points everywhere toward the "maw" i.e. towards the 2-regions of (Σ^*, b^*) whose orientation induces the *non* prevailing orientation on $\mathrm{Sing}(\Sigma^*)$;
- It has simple tangency points at $\partial\mathcal{N}$.

The closure of every component of $\Sigma^* \setminus \mathcal{N}$ is a 2-disk R. For every ∂R there is an even number $2t(R)$ of tangency points of the partial foliation μ already constructed. We define the index

$$d(R) = 1 - t(R) \ .$$

Then we can extend μ to a singular foliation defined on the whole of Σ^*. The singular set is contained in the set of intersection points x_R of the disks R with the dual edges in T. The smooth local model of μ at every such a point x_R is either like the vertical foliation at 0 of the quadratic differential $z^{-2d(R)}dz^2$, or is given by the gradient of $\pm(x^2 + y^2)$. Hence x_R is singular for μ if and only if $d(R) \neq 0$. Let us call μ the *maw foliation* of Σ^* (hence on Σ); it is uniquely determined up to homotopy through foliations having the same properties along $\mathrm{Sing}(\Sigma^*)$ and at the points x_R's. Notice that

$$\chi(M) = \frac{1}{2}\chi(\partial M) = \sum_{R \in \Sigma^{(2)}} d(R)$$

moreover, the cellular cochain $E(\Sigma, b) \in C^2(\Sigma; \mathbb{Z})$ which assigns the value $d(R)$ to every (R, b) as above, represents the Euler class of the oriented 2-plane distributions associated to $\mathcal{H}$.

(2) Take a normal embedding $M \subset F(T, b)$ We can consider now the singular foliation $\hat{\mu}$ of $F = F(T, b)$ whose leaves are of the form $l \times t$, l being a leaf of μ. Hence for every singular point x of μ, there is the vertical singular segment $\{x\} \times I$ of $\hat{\mu}$. Let $(\mathcal{V}, \mathcal{H})$ be a couple of vertical/horizontal foliations of M constructed sofar. For every singular point x of μ, the leaf $\{x\} \times I \subset M^\circ$, and has endpoints which belong to boundary leaves of both $\mathcal{H}^*$ and $\mathcal{H}$. Then $\hat{\mu}$ "restricts" to every component of $\partial M \setminus \mathcal{U}_\mathcal{V}$. This extends to a singular foliation $\partial_s\mu$ (called the *singular boundary maw foliation*) of the whole of ∂M whose singular set consists of the union of the isolated maw singular points with the tangency

line $X = X_\mathcal{V}$. Finally the *boundary maw* $\partial\mu$ is obtained by inverting the $\partial_s\mu$ orientations on the white components of the bicoloring $\partial\mathcal{V}$ of ∂M. It turns out that the orientation conflict disappears at every component C of $X_\mathcal{V}$ and eventually $\partial\mu$ is traversing every annulus $\mathcal{U}_C$ without boundary tangency points, and only the isolated maw singular points survive; $\partial\mu$ is uniquely determined up to homotopy through foliations positively transverse to $X_\mathcal{V}$ and which are isotopic at the singular points. Finally we can state

Proposition 7.1. *The singular foliation $\partial\mu = \partial\mu_{T,b}$ coincides with the vertical foliation carried by $(\partial\tilde{T}, \partial\omega_b)$.*

Essentially this holds 'by construction'; we omit the details of the verification. Now we can characterize the elementary non ambiguous ideal b-transits in terms of a preserved boundary configuration; the invariance of the maw besides the boundary bicoloring characterizes the non ambiguous within the whole set of sliding transits.

Proposition 7.2. *Let $(T,b) \to (T',b')$ be an ideal ($2 \leftrightarrow 3$ or $0 \leftrightarrow 2$) b-transit. Then the following facts are equivalent to each other:*

(1) It is non ambiguous;

(2) $(\partial\mathcal{V}, \partial\mu)_{(T,b)} = (\partial\mathcal{V}, \partial\mu)_{(T',b')}$ up to isotopy.

Moreover, $(\partial\mathcal{V}, \partial\mu)_{(T,b)}$ is invariant under the non ambiguous ideal branched equivalence.

This can be checked case by case.

We are going to finish by pointing out a further branched *na* invariant based on the horizontal foliation $\mathcal{H} = \mathcal{H}_{T,b}$. We denote by $H_2^C(\Sigma; \mathbb{R})$ the cellular singular homology, provided that every region of the spine Σ is oriented by the branching b. Then $H_2^C(\Sigma; \mathbb{R})$ is isomorphic to the singular homology $H_2(M; \mathbb{R})$ and coincides with the space of 2-cycles $Z_2^C(\Sigma; \mathbb{R})$. Every $z \in Z_2^C(\Sigma; \mathbb{R})$ consists in giving each b-oriented region R of Σ a weight $z(R) \in \mathbb{R}$ in such a way that the three weights around every edge of $\mathrm{Sing}(\Sigma)$ verify a switching condition of the form $z(e_0) = z(e_1) + z(e_2)$. These cycles transit along every ideal b-transit, so that for every composite b-transit $(T,b) \Rightarrow (T',b')$ it is defined an isomorphism

$$\alpha : Z_2^C(\Sigma; \mathbb{R}) \to Z_2^C(\Sigma'; \mathbb{R}) \ .$$

Set

$$\mathcal{M} = \mathcal{M}_{(T,b)} = \{z \in Z_2^C(\Sigma; \mathbb{R}) |\ \forall R,\ z(R) \geq 0\}; \ \mathcal{M}^+ = \{z \in Z_2^C(\Sigma; \mathbb{R}) |\ \forall R,\ z(R) > 0\} \ .$$

Every $z \in \mathcal{M}$ can be interpreted as a *transverse measure* on the horizontal foliation $\mathcal{H}$. By taking into account the arbitrary choices in the realizations of $\mathcal{H}$) we radily have

Proposition 7.3. *(1) For every $z \in \mathcal{M}$, the measured foliation $(\mathcal{H}, z)$ is uniquely detemined up to measure equivalence.*
(2) If we denote by $\mathcal{M}(\mathcal{H})$ the set of transverse measures on $\mathcal{H}$ up to measure equivalence, then the above correspondence well defines a map

$$\mathfrak{m} = \mathfrak{m}_{(T,b)} : \mathcal{M}_{(T,b)} \to \mathcal{M}(\mathcal{H}) \ .$$

$\square$

After a look at the *na*-transits we readily have

Proposition 7.4. *If (T,b) and (T',b') are na-transit equivalent, then the maps $\mathfrak{m}_{(T,b)}$ and $\mathfrak{m}_{(T',b')}$ have the same image. More precisely, there is a bijection $\alpha : \mathcal{M}_{(T,b)} \to \mathcal{M}_{(T',b')}$ such that $\alpha(\mathcal{M}_{(T,b)}^+) = \mathcal{M}_{(T',b')}^+$ and $\mathfrak{m}_{(T,b)} = \mathfrak{m}_{(T',b')} \circ \alpha$.*

$\square$

References

[1] I. Agol, *Ideal Triangulations of Pseudo-Anosov Mapping Tori*, in *Topology and geometry in dimension three*, Amer. Math. Soc. Contemp. Math. Vol 560 (2011), 1–17

[2] I. Altman, S. Friedl, A. Juhsz, *Sutured Floer homology, fibrations, and taut depth one foliations*, Trans. Amer. Math. Soc. 368 (2016), 6363-6389.

[3] G. Amendola, *A calculus for ideal triangulations of three-manifolds with embedded arcs*, Math.Nachr. 278 (2005), no. 9, 975-994.

[4] S. Baseilhac, R. Benedetti, *On the quantum Teichmüller invariants of fibred cusped 3-manifolds* , Geometriae Dedicata, 197(1), 1–32 , 2018.

[5] S. Baseilhac, R. Benedetti, *Non ambiguous structures on* 3-*manifolds and quantum symmetry defects*, Quantum Topology, Volume 8, Issue 4, 2017, pp. 749–846.

[6] S. Baseilhac, R. Benedetti, *Analytic families of quantum hyperbolic invariants*, Algebraic and Geometric Topology, 15 (2015) 1983 − 2063.

[7] R. Benedetti, *On ideal triangulations of surfaces up to branched transit equivalences*, preprint on arXiv 2019.

[8] R. Benedetti, C. Petronio, *Spin structures on* 3-*manifolds via arbitrary triangulations*, Alg. Geom. Topol. 14 (2014) 1005–1054.

[9] R. Benedetti, C. Petronio, *Reidemeister-Turaev torsion of 3-dimensional Euler structures with simple boundary tangency and pseudo-Legendrian knots*, Manuscripta Math. 106 (1) (2001) 13–61.

[10] R. Benedetti, C. Petronio, *Combed 3-manifolds with concave boundary, framed links, and pseudo-Legendrian links*, Journal of Knot Theory and its Ramifications 1,10 (2001), 1–35.

[11] R. Benedetti, C. Petronio, *Branched Spines and Contact Structures on 3-manifolds*, Ann. Mat. Pura Appl. (4) 178 (2000), 81–102.

[12] R. Benedetti, C. Petronio, *Branched Standard Spines of* 3-*manifolds*, Lect. Notes Math. 1653, Springer (1997).

[13] F. Costantino, *A calculus for branched spines of 3-manifolds*, Math. Zeitschrift 251 (2) (2005) 427–442.

[14] S Friedl, A Juhsz, J Rasmussen, *The decategorification of sutured Floer homology*, Journal of Topology, 2011.

[15] D. Gillman, D. Rolfsen, *The Zeeman conjecture for standard spines is equivalent to the Poincaré conjecture*, Topology Vol. 22, no. 3, (1983) 315–323.

[16] M. Lackenby, *Taut ideal triangulations of 3-manifolds*, Geom. Topol. 4 (2000) 369–395.

[17] A. Hatcher, *Algebraic Topology*, Cambridge University Press, 2002.

[18] S, Halperin, D. Toledo, *Stiefel-Whitney homology classes*, Ann. of Math. (2) 96 (1972), 511–525.

[19] I. Ishii, *Flows and spines*, Tokyo J. Math. 9 (1986) 505–525.

[20] A.Yu. Makovetski, *Transformations of special spines and special polyhedra*, Math. Notes 65 (1999), 295–301.

[21] G. Massuyeau, J-B. Meilhan, *Equivalence relations for homology cylinders and the core of the Casson invariant*, Trans. Amer. Math. Soc. 365 (2013), 5431-5502.

[22] S.V. Matveev, *Transformations of special spines, and the Zeeman conjecture*, Izv. Akad. Nauk SSSR Ser. Mat. 51 (1987), no. 5, 1104?1116, 1119.

[23] R. Piergallini, *Standard moves for standard polyhedra and spines*, Rend. Circ. Mat. Palermo (2) Suppl. (1988), no. 18, 391?414, Third National Conference on Topology (Trieste, 1986).

[24] J. H. Rubistein, H. Segerman, S. Tillmann *Traversing three-manifold triangulations and spines*, arXiv:1812.02806v1 [math. GT] 6 Dec 2018.

Dipartimento di Matematica, Largo Bruno Pontecorvo 5, 56127 Pisa, Italy

E-mail address: riccardo.benedetti@unipi.it